

AN EXPERIMENTAL AND ANALYTICAL METHOD FOR
APPROXIMATE DETERMINATION OF THE TILT
ROTOR RESEARCH AIRCRAFT
ROTOR/WING DOWNLOAD

c/s CB 609194

FINAL REPORT

PRINCIPAL INVESTIGATORS

David E. Jordon

William Patterson

Doral R. Sandlin

05/30/84 - 11/30/85

California Polytechnic State University
Aeronautical Engineering Department
San Luis Obispo, California

Grant No. NCC2-259

(NASA-CR-176970) AN EXPERIMENTAL AND
ANALYTICAL METHOD FOR APPROXIMATE
DETERMINATION OF THE TILT ROTOR RESEARCH
AIRCRAFT ROTOR/WING DOWNLOAD Final Report,
30 May 1984 - 30 Nov. 1985 (California)

N86-29769

Unclassified
G3/02 43236

ABSTRACT

AN EXPERIMENTAL AND ANALYTICAL METHOD FOR
APPROXIMATE DETERMINATION OF THE TILT
ROTOR RESEARCH AIRCRAFT
ROTOR/WING DOWNLOAD

David E. Jordan

May 1986

An investigation was performed to analyze the XV-15 Tilt Rotor Research Aircraft download phenomenon. This phenomenon is a direct result of the two rotor wakes impinging on the wing upper surface when the aircraft is in the hover configuration. This study represents one of many devoted to the analysis of this problem.

For this study the analysis proceeded along two lines. First was a method whereby results from actual hover tests of the XV-15 aircraft were combined with drag coefficient results from wind tunnel tests of a wing that was representative of the aircraft wing. Second, an analytical method was used that modeled the airflow caused by the two rotors. Formulas were developed in such a way that a computer program could be used to calculate the axial velocities in the vicinity of the aircraft's wing. The axial velocities were then used in conjunction with the aforementioned wind tunnel drag coefficient results to produce download values. An attempt was made to validate the analytical results by modeling a model rotor system for which direct download values were determinable.

Table of Contents

	Page
List of Tables	v
List of Figures	vi
List of Symbols	viii
Chapter	
1. Introduction	1
Description	1
History	4
2. Experimental Determination of the Download .	9
Hover Test	9
Wind Tunnel Tests	20
Experimental Download Analysis	22
3. Analytic Determination of the Download	28
Vortex Ring Induced Velocity	29
Wake Contraction	33
Time Spacing of Vortex Rings	35
Analytic Download Analysis	36
Computer Program Calibration	39
Download Computer Program	41
Velocity Profiles	44
4. Model Test	49
5. Results and Discussion	51
Experimental Download Analysis	51

Chapter		Page
5. (continued)		
Model Test Analysis	55	
Analytic Download Analysis	56	
6. Conclusion	63	
References	66	
Appendixes		
A. Transformation from Equation 6 to Equation 7	68	
B. Empirical Adjustment to Power Polar to Reflect Nonlinear Aerodynamics Region . . .	70	
C. Development of the Biot-Savart Equation to Determine the Axial Velocity Component Due to a Vortex Ring	73	
D. Calibration Version of XV-15 Computer Program	82	
E. Download Version of XV-15 Computer Program	88	
F. Calibration Version of Model Rotor Computer Program	100	
G. Download Version of Model Rotor Computer Program	106	

Tables

Table	Page
1. Out of Ground Effect Full Span Flap Hover Data	12
2. Deviation of C_w From Linear C_p Vs. $C_w^{3/2}$ Relationship	20
3. Rotor Lifted Weights and Flap Deflection Angles at a Constant Power Setting	21
4. Drag Coefficients and Flap Deflection Angles	23
5. Experimental Download	24
6. Analytic Download	58

Figures

Figure	Page
1. The XV-15 Tilt Rotor Research Aircraft	2
2. XV-15 Flap/Flaperon Schedule	10
3. XV-15 Engine Exhaust Jet Thrust	13
4. XV-15 Power Coefficient/Weight Coefficient Polar	18
5. Weight Coefficient Deviation From Linear Aerodynamics as a Function of Power Coefficient	19
6. XV-15 Experimental Power Coefficient/ Weight Coefficient Polar	19
7. Effect of Flap Angle Deflection on Rotor Lifted Weight	21
8. Effect of Flap Angle Deflection on Two- Dimensional Drag Coefficient	23
9. Effect of Flap Angle on Drag Coefficient Change, Referenced to the Drag Coefficient for 0° Flap Deflection	25
10. Change in Rotor Lifted Weight, Referenced to Rotor Lifted Weight for 0° Flap Deflection, as a Function of the Change in Drag Coefficient	26
11. Experimental XV-15 Download As a Function of Flap Deflection Angle	27
12. The Geometry Used for Deriving the Axial Velocity Component Due to a Vortex Ring	30
13. Vortex Ring Downstream Position as a Function of Time	38
14. In Ground Effect Vortex Ring Representation	43
15. Computer-Generated Velocity Profile, $C_t = .0094$	46

Figure	Page
16. Computer-Generated Velocity Profile, $C_t = .01$	47
17. Computer-Generated Velocity Profile, $C_t = .0105$	48
18. Model Rotor Test Setup	49
19. Effect of Hover Height on Analytic XV-15 Download	58

Symbols

- A_D : rotor disk area (ft.²)
 C_d : drag coefficient
 C_p : power coefficient
 C_{p_o} : profile power coefficient
 C_t : thrust coefficient
 C_w : weight coefficient
 c : wing chord (ft.)
DL: aircraft rotor/wing download (lb.)
DL/T: aircraft download-to-thrust ratio
 δ_f : flap deflection angle (deg.)
 F_j : engine exhaust jet thrust (lb.)
GW: aircraft gross weight (lb.)
 r : circulation strength (ft.²/sec.)
H/D: rotor height above ground to rotor diameter ratio
IGE: in ground effect hover
K: vortex ring time spacing factor
OGE: out of ground effect hover
R: rotor radius (ft.)
 r' : vortex ring radius (ft.)
 ρ : ambient air density (slugs/ft.³)
STOL: short take-off and landing
T: rotor thrust (lb.)
VTOL: vertical take-off and landing

Symbols (continued)

v_i: average induced velocity at the rotor disk
(ft./sec.)

v_t: rotor tip speed (ft./sec.)

w: aircraft rotor lifted weight (lb.)

CHAPTER 1

Introduction

Description

The XV-15 (Figure 1) is a "Tilt-Rotor" aircraft. The aircraft has a wingspan of 32 feet 2 inches, a length of 46 feet 3 inches, and a design gross weight of 13,000 pounds. The aircraft's propulsion system consists of two Lycoming LTC1K-4K turboprop engines and two 25-foot diameter, three-bladed prop-rotors. These engines are variants of Lycoming T53-L-13B engines and are mounted one on each wing tip. The rotor axes are capable of rotation from a vertical position (for helicopter and hover flight) to a horizontal position (for airplane flight). Control of the aircraft in the helicopter configuration is provided by rotor-generated forces and moments, while in the airplane configuration control is provided primarily by conventional control surfaces. Operation at engine tilt angles between vertical and horizontal provides short take-off and landing (STOL) capabilities, as opposed to vertical take-off and landing (VTOL) capabilities. Cross shafting of the two engines provides rotational speed synchronization, permits power transfer for transient conditions, and prevents complete loss of power to either rotor due to a single engine failure.

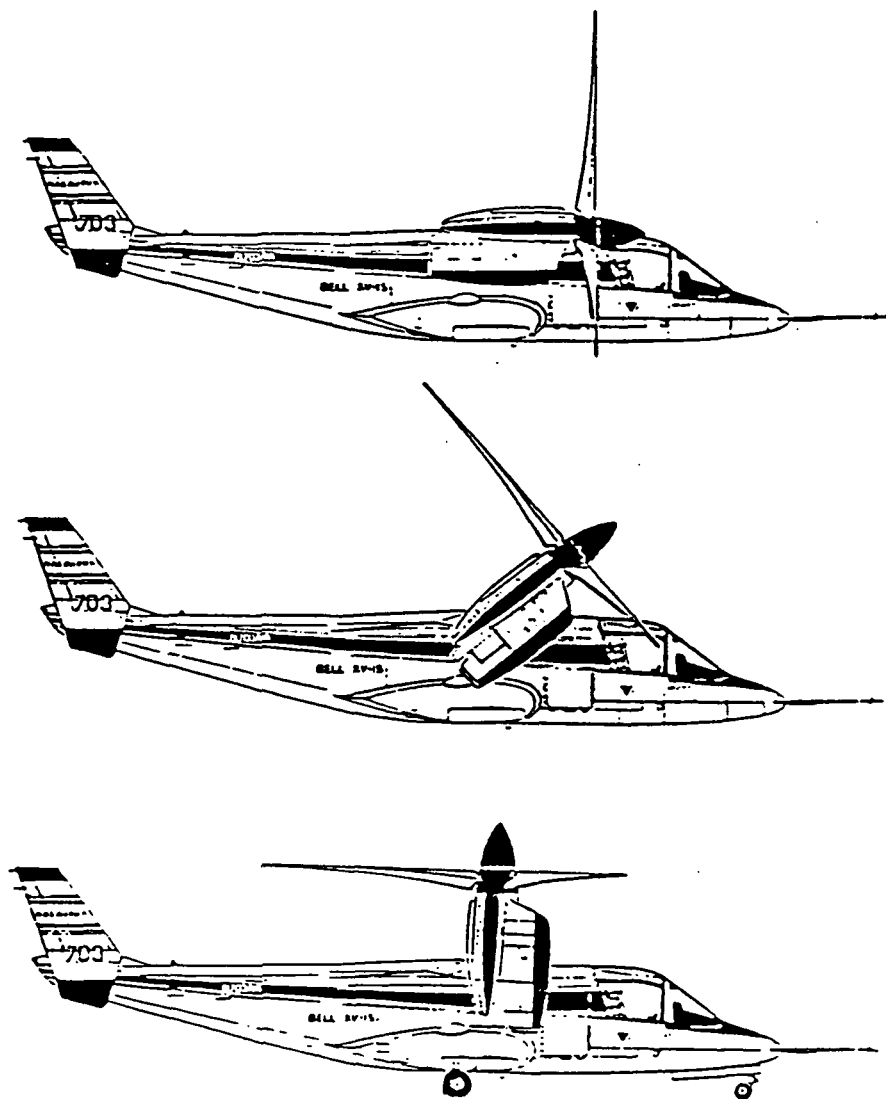


Figure 1
The XV-15 Tilt Rotor Research Aircraft

The XV-15 was designed and built as a "proof of concept" aircraft and is providing a data base for the larger scale V-22 Osprey that is currently in the preliminary design phase. Two XV-15 aircraft were built by Bell Helicopter Textron Inc. under contract by NASA. One, aircraft 702, was retained by Bell Helicopter and is operated in Texas; the other, aircraft 703, is operated by NASA at Ames Research Center.

The XV-15 tilt rotor research aircraft is a unique aircraft with unique capabilities. Along with the capabilities, however, come unique problems. One problem occurs when the aircraft is operating in a hover. In this configuration the engines are in a vertical position with the rotor disks parallel to the wing surface. The wing is approximately 5 feet below the rotor disk and experiences a "downward" directed force due to the direct impingement of the rotor wake on the wing. The approximate determination of the magnitude of this downward directed force, hereafter referred to as download, was the goal of this research project. The download and its elimination, or at least reduction, is a significant problem for today's XV-15 proof of concept prototype and tomorrow's V-22 Osprey production aircraft.

It is difficult to experimentally determine the aircraft download due to the number of variables involved: rotor thrust, engine exhaust jet thrust, aircraft gross weight, download, and upload in the case of a ground effect

reflected wake. The problem with the experimental determination of the download arises from the fact that there is no readily apparent way to separate the download out of a gross measurement of the vertical force system. While the aircraft gross weight can be exactly determined, the exhaust jet thrust can only be approximated, being a function of inlet air velocity, and the installed rotor thrust defies determination due to its direct interrelation with the download phenomenon. These facts have led to many attempts to determine download through model test and theoretical techniques.

History

The first record of a download type phenomenon was encountered in the late 1950s with the XV-3 (Deckert and Ferry, 1960). The XV-3 was a S/VTOL aircraft much like the XV-15 except that it was powered by one radial type piston engine mounted in the aircraft fuselage. Power was shafted to a transmission at each wing tip which drove two bladed prop-rotors.

During the flight test evaluations of the XV-3 it was discovered that a large increase in power required was encountered suddenly when hover flight was approached. This fact was attributed to an aspect ratio effect. The reasoning was that theoretically, above transitional speeds, the prop-rotors were actually influencing a diameter of air extending from the outboard edge of one prop-rotor to the outboard edge of the other. With this

large mass of air being influenced, the induced power required was necessarily low. However, below transitional speed (i.e., in hovering flight), each prop-rotor was thought to influence a diameter of air approximately equal to its own diameter. Thus, with the much smaller mass of air being influenced, the induced power requirement had to be increased to produce the same thrust. While this explanation seems feasible, the problem could have been the first encounter with tilt-rotor download.

In 1969 a test was conducted at Wright-Patterson Air Force Base that placed a mock-up under a full-scale CH-47 Chinook rotor (Gillmore, 1971). It was speculated that on a wing without leading or trailing edge devices the download force would approach 12% of the aircraft gross thrust. The test wing, however, was run utilizing trailing edge flaps deflected 70° in conjunction with a leading edge device that opened like an umbrella, top and bottom. Using this configuration it was demonstrated that the download could be reduced to 4% of gross thrust. While these results seem perfectly accurate and acceptable, the extension of these values to reflect the XV-15 would be questionable. The test used only one rotor and no image plane or end plate to simulate the longitudinal symmetry of the XV-15. Thus, the test did not adequately model the flow phenomenon that exists on the XV-15.

Other tests were conducted by the Bell Helicopter Company beginning in 1968 (Marr, Sambell, and Neal, 1973)

that utilized a 1/5 scale powered aeroelastic model of the XV-15. The model was tested at rotor height above ground to rotor diameter (H/D) ratios from 0.5 through 1.0. In an attempt to isolate the download force, the model was run both with and without wing panels installed. The test revealed that at an H/D value of 1.0 the wing panel download was 11.4% of the model thrust. This value was higher than the 7% that was predicted for the full-scale aircraft. It was thought that the difference between the predicted and actual values could be attributed to a Reynold's number effect. A Reynold's number correction had the effect of reducing the predicted download value to 5-7% of the full-scale thrust. The results of these tests are also suspect because of two factors. First, the Reynold's number correction was based on wind tunnel data of "cross sectional shapes with rounded edges and flat sides" and not the model aircraft wing. Second, the download predicted for the full-scale tilt rotor aircraft was based on in ground effect (IGE) data and therefore does not adequately reflect the general out of ground effect (OGE) solution.

The latest tests that addressed the download issue were performed at the Outdoor Aerodynamic Research Facility (OARF) at NASA-Ames Research Center in 1984 (McVeigh, 1985). The download aspect of the tests was specifically directed toward the V-22 Osprey program but it was felt that the results were applicable to this study. The tests consisted of a 25-foot diameter three-bladed prop-rotor

mounted with its axis of rotation parallel to the ground. This configuration precluded any influence that the ground would have had on the prop-rotor performance. The effect of the opposing prop-rotor was simulated by using a large image plane. A wing, complete with a 31% of wing chord full span flap and follower, was placed downstream of the rotor disk between the rotor axis and the image plane. The wing was instrumented to facilitate the measurement of forces and moments. The results of the test show that for a flap deflection angle of 67° and a nominal design thrust coefficient of .016, the download-to-thrust ratio was 9.3%. The wing used for the tests had a chord of 10.5 feet and was placed approximately 8 feet downstream of the rotor disk with a 6° dihedral. This test represents the most recent and most accurate work done to date attempting to resolve the download issue.

The above tests show that the download problem is significant and deserves attention. The fact that early estimates of the download were in the 3% to 5% range but have grown to 9% to 10% of gross thrust is significant in itself. Applied to a hovering XV-15 aircraft, the difference in the early and late estimates of download account for a difference of almost 1,000 pounds.

The download analysis, for this study, was performed utilizing two different procedures. The first method was an experimental method that combined results from actual aircraft hover tests of the XV-15 and results of wind

tunnel tests of a model XV-15 wing. The second method was a computer simulation of the aircraft propulsion system, namely two 25-foot diameter prop-rotors, that relied on vortex ring theory. This method also made use of the same wind tunnel test results.

CHAPTER 2

Experimental Determination of the Download

Hover Test

Flight tests were utilized to attempt to experimentally determine the XV-15 rotor/wing download. A hover test was conducted in 1983 in which the aircraft was flown using five different deflection settings with careful attention to maintain the aircraft gross weight within a narrow range (approximately 13,500 to 13,700 pounds). Data from the hover test was utilized in conjunction with data acquired from wind tunnel tests of a representative two-dimensional airfoil to arrive at values of download-to-thrust ratio.

The XV-15 aircraft wing is equipped with a flap/flaperon control surface system. The system is rigged to provide a linear relationship between the flap and flaperon deflection, i.e., a flap deflection of 40° causes a flaperon deflection of 25°, a flap deflection of 20° causes a flaperon deflection of 13°, etc. (Figure 2). Throughout this linear deflection relationship, roll control is accomplished by the pilot's flaperon input overriding the associated flap/flaperon angle relationship. The flaperon deflection, corresponding to the pilot input, is from the position predetermined by the flap setting. For the hover download investigation, a special modification was implemented to

the flap/flaperon system which facilitated ground adjustment of the flaps and flaperons to the same deflection angle, thereby producing the effect of a full span flap system (Figure 2). The deflection angles used during the test for the full span flap system were 0° , 20° , 40° , 50° , and 60° .

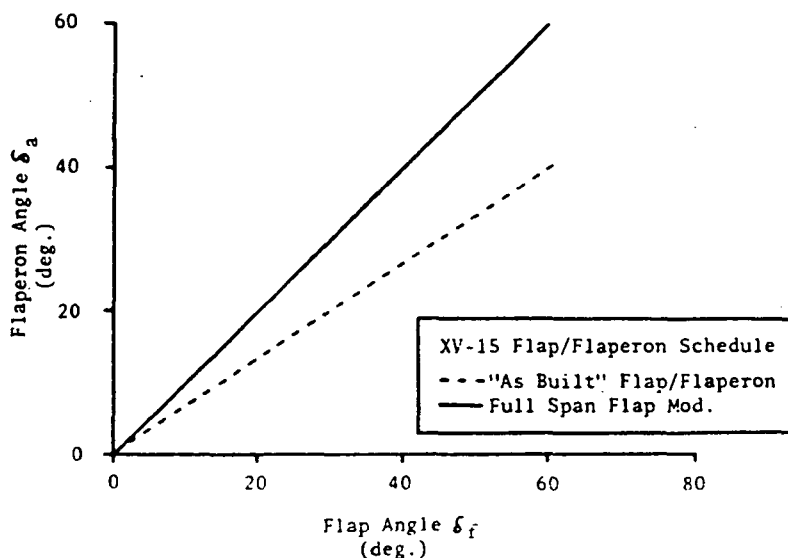


Figure 2
XV-15 Flap/Flaperon Schedule

In order to facilitate a direct correlation between test points throughout the hover test, efforts were made to keep the aircraft gross weight within a narrow range. Ballast was added to the aircraft during the flap readjustment ground time to compensate for the fuel burned during each portion of the test. Accordingly, the aircraft gross weight was maintained within a 200-pound range. Aircraft gross weight determination during the test sequences was

performed after the tests using on-board fuel quantity instrumentation data.

An aircraft wheel hover height of 50 feet above the ground was established for the tests using visual references. This height corresponds to an H/D ratio of 2.5, insuring that the data taken would represent OGE conditions.

Rotor speeds were held constant (± 1 RPM) throughout the test points through the use of the engine RPM governor. Three data points per flap setting were recorded and are presented in Table 1. Ambient test conditions were monitored and recorded through the use of a local weather station that was placed well outside of the rotor influence. Light winds existed throughout the test period ranging from 2.5 knots at 320/045° to 4 knots at 340°. The aircraft heading was held constant at 320° during the tests.

The system of vertical forces that act on the XV-15 during hover operation is composed of four components: engine exhaust jet thrust, rotor thrust, aircraft gross weight, and the rotor/wing download.

Engine jet thrust was determined with an acceptable degree of accuracy using Lycoming LTC1K-4K engine data (Figure 3). Engine exhaust jet thrust is dependent on engine horsepower and free stream velocity in the vicinity of the engine inlet. After the rotor tip speed and mast torque were determined from aircraft instrumentation, rotor horsepower could be calculated. Assuming that the

Table 1
Out of Ground Effect Full Span
Flap Hover Data

RECORD	FLAP (DEG)	GROSS WT (LBS)	WIND (V _K /DIRECT)	σ	ROTOR SPEED (RPM)	MAST TORQUE (WLB) LEFT	RIGHT
534	0	13550	2.5/045°	.9917	587	116814	118841
535	0	13536	2.5/045°	.9917	587	114808	116764
536	0	13527	2.5/045°	.9917	587	115728	118494
537	20	13537	3.5/340°	.9917	587	112384	114652
538	20	13521	3.5/340°	.9917	587	113043	114092
539	20	13513	3.5/340°	.9917	587	114356	115005
540	40	13657	3.0/345°	.9955	587	111464	113951
541	40	13647	3.0/345°	.9955	587	111305	114479
542	40	13637	3.0/345°	.9955	587	110827	115429
543	50	13673	3.0/340°	.9917	587	109476	112615
544	50	13662	3.0/340°	.9917	587	108636	111456
545	50	13645	3.0/340°	.9917	587	109314	113052
547	60	13614	4.0/340°	.9936	588	107176	118768
548	60	13601	4.0/340°	.9936	588	108460	108746
549	60	13585	4.0/340°	.9936	587	105907	109352

Parameters							
RECORD	AVG. SHAFT POWER (HP)	C _P	\bar{C}_P	ENGINE JET THRUST (LBS)	C _w (NON (GW-2F) LINEAR)	$\bar{C}_w^{3/2}$	\bar{C}_w (LINEAR)
534	1098	.001150		85.0	13380	.00979	
535	1079	.001130	.001141	83.5	13369	.00978	.000967 .01007
536	1091	.001143		84.0	13359	.00977	
537	1057	.001108		83.0	13371	.00978	
538	1058	.001108	.001112	83.0	13355	.00977	.000966 .010043
539	1068	.001119		83.0	13347	.00977	
540	1050	.001095		82.5	13492	.00983	
541	1052	.001097	.001097	83.0	13481	.00982	.000973 .01006
542	1054	.001099		83.0	13471	.00981	
543	1034	.001083		82.0	13509	.00988	
544	1025	.001074	.001080	81.7	13499	.00989	.000982 .010107
545	1036	.001084		82.0	13481	.00986	
547	1008	.001048		81.0	13454	.00979	
548	1013	.001054	.001050	81.5	13438	.00978	.000969 .009987
549	1003	.001048		80.2	13425	.00980	

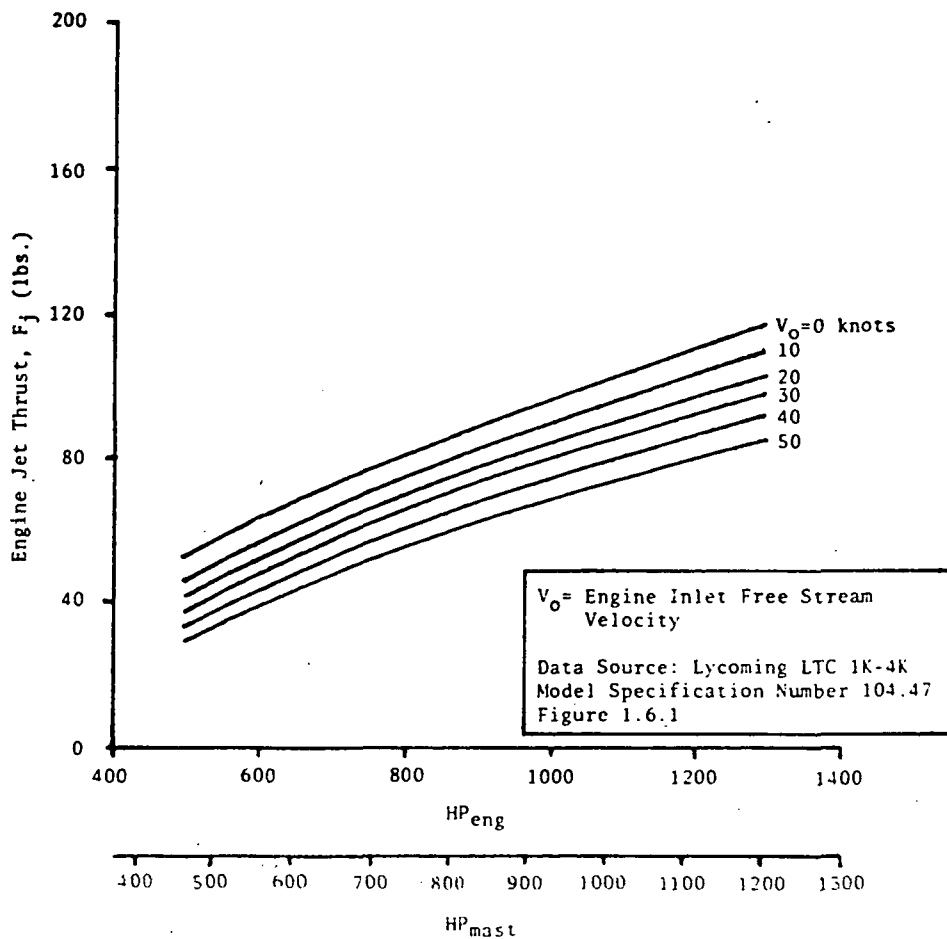


Figure 3
XV-15 Engine Exhaust Jet Thrust

transmission linking the engine and rotor was 93% efficient, calculation of the engine horsepower was then possible. Computation of the free stream velocity in the vicinity of the engine inlet was accomplished through the use of simple momentum theory (i.e., $v_i = v_t \sqrt{C_t/2}$). In order to determine the aircraft thrust coefficient, the thrust per rotor was assumed to be 110% of half the aircraft gross weight and the rotor tip speed was determined

from aircraft instrumentation. These two values facilitated calculation of the average rotor-induced velocity. This value of average rotor-induced velocity was assumed to approximately represent the free stream velocity in the vicinity of the engine inlet. With the induced velocity and engine horsepower determined, a first approximation of engine exhaust jet thrust was possible. Further iterations to refine the engine exhaust jet thrust values were deemed unnecessary due to the apparent insensitivity of the jet thrust to the level of rotor thrust and also the relatively small value that the jet thrust represented compared to the other forces in the system. Engine jet thrust during the hover tests was determined to be between 80 and 85 pounds per engine. Doubling this value accounted for the total engine exhaust jet thrust. This total engine exhaust jet thrust was then subtracted from the aircraft gross weight and the value that resulted represented the "rotor lifted" aircraft weight (i.e., $W = GW - 2F_j$).

The rotor lifted aircraft weight was used to define a "weight coefficient." This weight coefficient was in the form of the standard helicopter thrust coefficient, with half of the total rotor lifted weight substituted for the rotor thrust. The form of the weight coefficient was

$$C_w = \frac{GW - 2F_j}{2\rho A_D V_t^2} \quad (1)$$

In order to be able to apply the OGE hover test data at other levels of power coefficient (C_p), the $C_p = mC_t^{3/2} + C_{p_0}$ power polar algorithm (Hayden, 1976), applicable only in the linear aerodynamic range, was utilized. This algorithm expresses the total power coefficient as being composed of the induced power, which is proportional to the thrust coefficient to the three halves power, and the profile power, which is that power required to turn the rotor in a zero thrust condition. Although this is an approximation, for hovering flight the combination of induced and profile power accounts for 90% to 100% of the total power.

Solving the algorithm for thrust coefficient (C_t) gives:

$$C_t = \left(\frac{C_p - C_{p_0}}{m} \right)^{2/3} \quad (2)$$

Calculating the slope (m) between a general point $(C_{p_1}, C_{t_1}^{3/2})$ and the C_p intercept $(0, C_{p_0})$ gives:

$$m = \frac{C_{p_1} - C_{p_0}}{C_{t_1}^{3/2}} \quad (3)$$

Substituting this expression into that for C_t gives:

$$C_t = \left(\frac{C_p - C_{p_0}}{\frac{C_{p_1} - C_{p_0}}{C_{t_1}^{3/2}}} \right)^{2/3} \quad (4)$$

where $(C_{p_1}, C_{t_1}^{3/2})$ is a general OGE hover point corresponding to a given flap setting and C_{p_0} is the C_p axis intercept of

the $C_t = mC_t^{3/2} + C_{p_0}$ curve, which is based on prior XV-15 hover data (Hoerner, 1965). Referring back to the relationship that the rotor lifted weight is equal to the aircraft gross weight less the engine exhaust jet thrust plus the rotor/wing download gives

$$T = W + DL \quad (5a)$$

or

$$T = W \left[1 + \frac{DL}{W} \right] \quad (5b)$$

Dividing through by the density, rotor disk area and rotor tip speed squared ($\rho A_D v_t^2$) gives:

$$C_t = C_w \left[1 + \frac{DL}{W} \right] \quad (6)$$

Using the manipulation outlined in Appendix A and substituting this final result into the previous relationship for thrust coefficient (C_t) gives:

$$C_t = C_w \left[1 - \frac{DL}{T} \right]^{-1} \quad (7)$$

Due to the fact that it has been shown (Makofski and Menkick, 1956) that the rotor/wing download to rotor thrust (DL/T) ratio is independent of the rotor disk loading but dependent on body configuration in the rotor wake alone, this ratio for the XV-15 is assumed to be dependent on flap configuration only. Thus $(1 + DL/T)$ was assumed to have a constant value for each flap angle setting and the expression for C_t derived from the power polar expression became:

$$C_{w_{\delta_f}} = \left[\frac{C_p - C_{p_0}}{C_{p_1} - C_{p_0}} \right]^{2/3} (C_{w_{\delta_{f1}}}) \quad (8)$$

This relationship, depicted in Figure 4, states that the rotor lifted aircraft weight (W) is, for a specific flap setting, only a function of applied power, C_p . Therefore, for each flap setting and its associated C_{p_1} and C_{w_1} values, a unique C_w value will be defined. From this it follows that for each unique C_w there will be a unique W , or rotor lifted aircraft weight. This relationship is particularly useful due to the fact that weight coefficient (C_w) values were easily obtainable from the hover test data (Table 1) while true thrust coefficient values could not be initially determined. The linear relationship of the $C_p = mC_t^{3/2} + C_{p_0}$ expression is applicable only for values of C_p below .0008, as can be seen in Figure 5. The deviation of C_w from the linear C_p vs. $C_w^{3/2}$ relationship is presented in Figure 6. At values of C_p above .0008, which is the case with the OGE hover data taken for this study, an empirical adjustment was utilized to reflect the departure from linear aerodynamics (Table 2). This adjustment consisted of finding a C_p dependent ΔC_w value from Figure 6, utilizing the study values of \bar{C}_p . This ΔC_w was then added to the nonlinear \bar{C}_w values to arrive at the associated C_w on the C_p vs. $C_w^{3/2}$ linear projection. A new value of C_w , at the desired C_p , is then obtained by interpolation (using the linear equation, Equation (8)). A second adjustment was then made to project the interpolated C_w back to the nonlinear C_p vs. $C_w^{3/2}$ curve. The second ΔC_w value was obtained from Figure 6 at the desired C_p

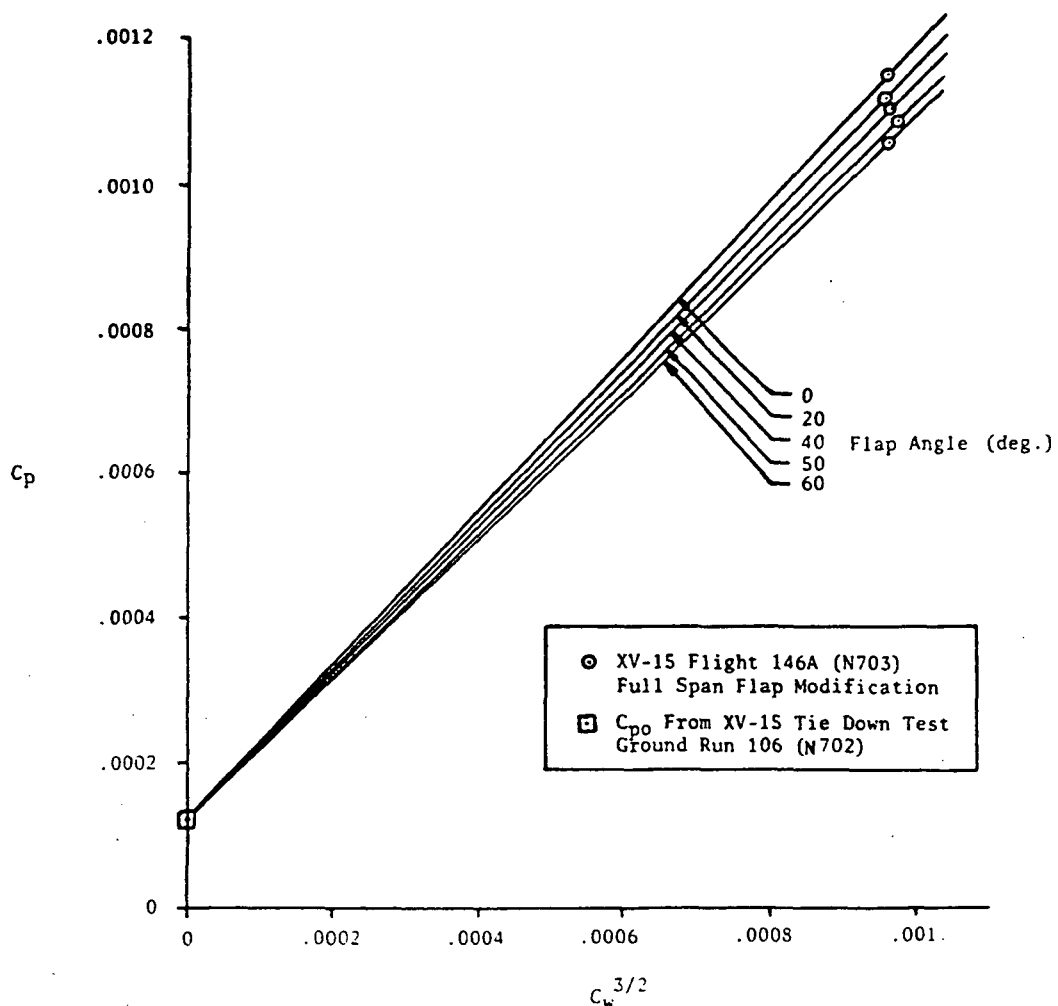


Figure 4

XV-15 Power Coefficient/Weight
Coefficient Polar

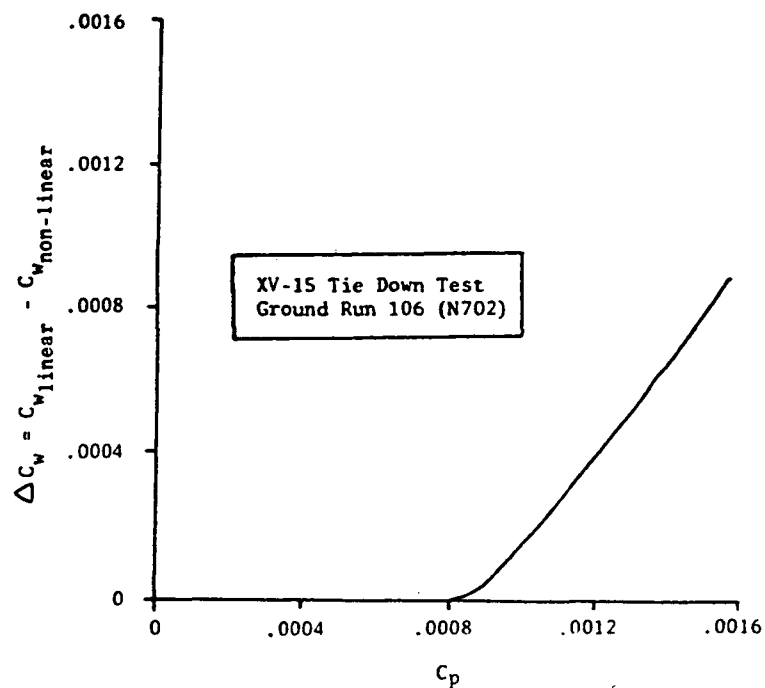


Figure 5

Weight Coefficient Deviation From Linear Aerodynamics as a Function of Power Coefficient

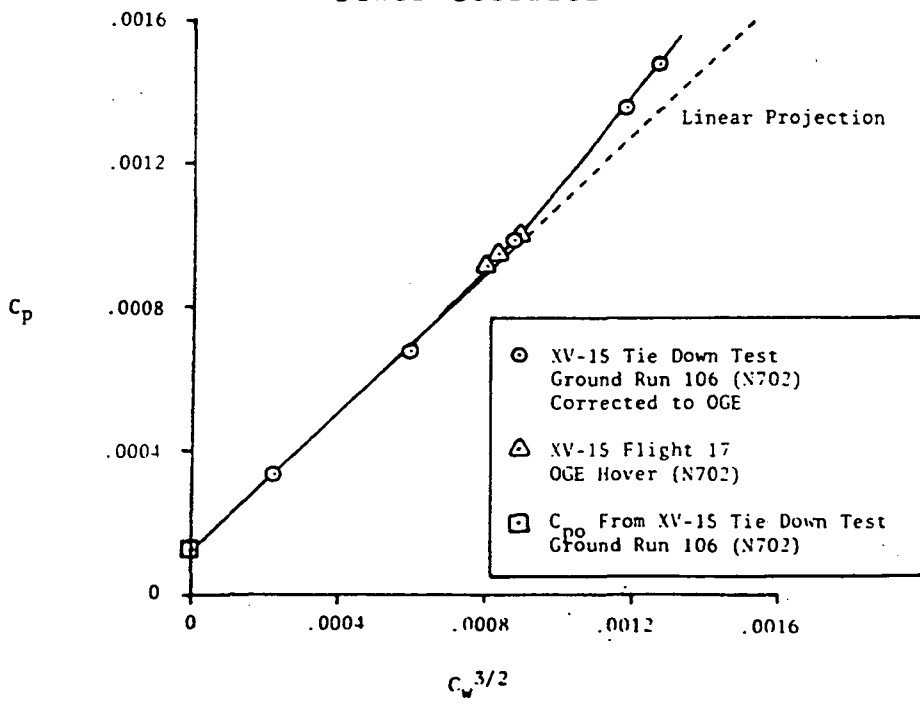


Figure 6

XV-15 Experimental Power Coefficient/Weight Coefficient Polar

Table 2
 Deviation of $C_w^{3/2}$ From Linear C_p Vs. $C_w^{3/2}$
 Relationship

C_p	$C_w^{3/2}$ UN	$C_w^{3/2}$ ACT	C_w UN	C_w ACT	C_w
.0008	.0007	.0007	.00788	.00788	0
.0009	.000808	.000796	.00867	.00859	.00008
.0010	.000908	.000888	.00938	.00924	.00014
.0011	.001012	.000972	.01008	.00981	.00027
.0012	.001114	.001055	.01075	.01036	.00038
.0013	.001215	.001134	.01139	.01087	.00051
.0014	.001316	.001212	.01201	.01137	.00064
.0015	.001418	.001283	.01262	.01181	.00081

(.001). Utilizing this method, outlined in Appendix B, computed values of C_w and W were determined and are presented, with the associated flap angle test points, in Table 3. The incremental weight (ΔW) column in Table 3 reflects the additional weight, referenced to the 0° flap angle weight, that could be hovered OGE as a result of increased flap angle deflection. The effect of flap angle on rotor lifted weight (ΔW) is presented in Figure 7.

Wind Tunnel Tests

Wind tunnel tests of two-dimensional wing sections were performed in the Army 7-foot by 10-foot wind tunnel at NASA Ames Research Center during April and May of 1983. The wind sections utilized plain flap configurations and were tested at angles of attack near -90°. Flaps of various chord sections were tested.

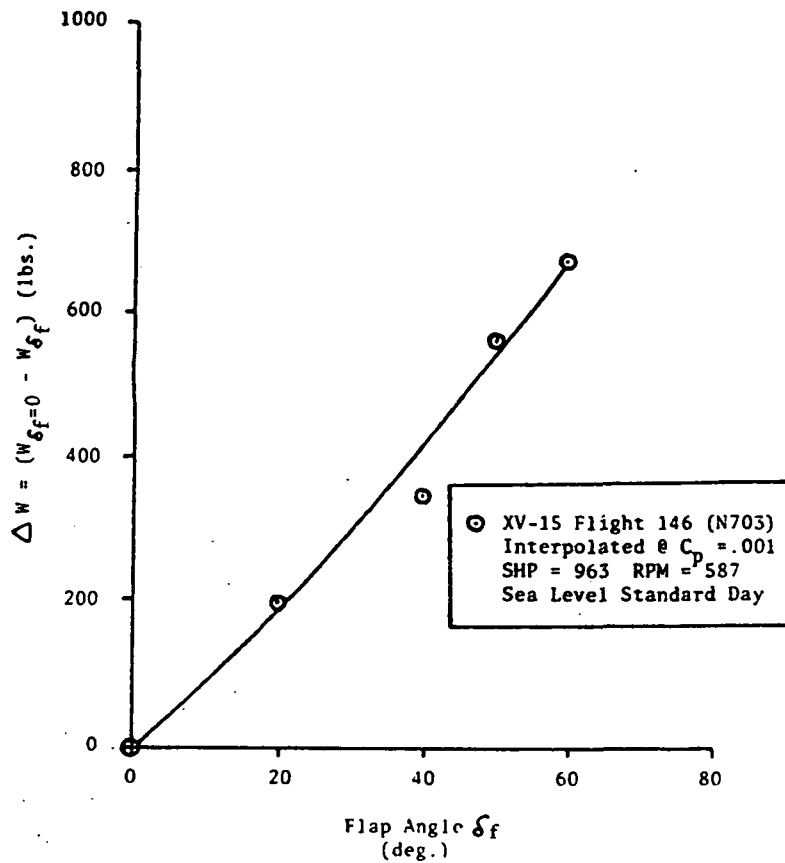


Figure 7

**Effect of Flap Angle Deflection on
Rotor Lifted Weight**

Table 3

**Rotor Lifted Weights and Flap Deflection
Angles at a Constant Power Setting**

δ_f (DEG)	$(@C_p = .001)$	W (GW-2F _j) (lbs.)	ΔW ($W_{\delta f=0} - W_{\delta f}$) (lbs.)
0	.00897	12,261	0
20	.00912	12,466	205
40	.00923	12,665	404
50	.00939	12,835	574
60	.00948	12,983	722

The variation of drag coefficient with flap angle for the various flap chords tested is presented in Figure 8. The decrease in drag coefficient with increasing flap deflection angle is interrupted by a sharp rise, reflecting the onset of separated flow on the flap upper surface. The wing section with the .25c flap, which is the same size flap as that on the XV-15, demonstrated flow separation characteristics about 10° earlier than observed on the aircraft. The cause of this could be traceable to the fact that the XV-15 flap is slightly thicker than that which would be dictated by the basic airfoil contour. The result of the greater flap thickness is a larger flap leading edge radius than that which was built into the wind tunnel flap. Since the drag coefficient characteristics for each of the flap chords tested were similar in the attached flow region, it was assumed that the XV-15 wing drag coefficients could be represented by extrapolation of the .25c flap data to 60° flap deflection, based on the performance characteristics of the .30c and .35c flaps. The extrapolation is shown as a broken line in Figure 8 and is included in Table 4.

Experimental Download Analysis

The ΔC_d values listed in Table 4 represent drag coefficient decreases, referenced to the 0° flap deflection drag coefficient, for each increase in flap deflection. The relationship of ΔC_d to flap deflection angles is

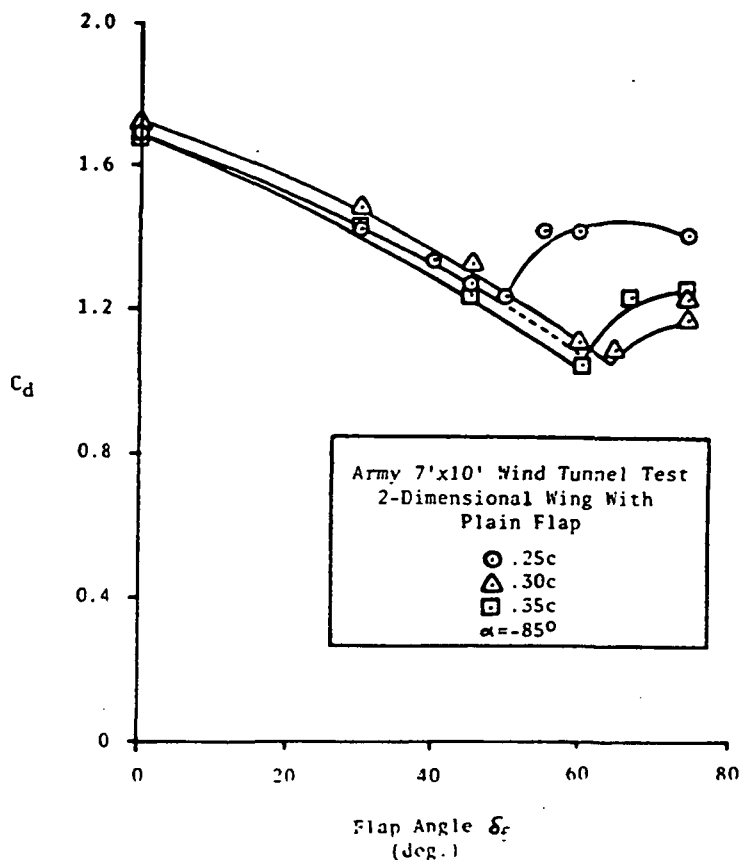


Figure 8

Effect of Flap Angle Deflection on Two-Dimensional Drag Coefficient

Table 4

Drag Coefficients and Flap Deflection Angles

δ_f (DEG)	C_d	$(C_d \text{ at } \delta_f = 0) - C_d \text{ at } \delta_f$
0	1.69	0
20	1.53	0.16
40	1.32	0.37
50	1.21	0.48
60	1.09*	0.60

*Extrapolated

depicted in Figure 9. Realizing that the decrease in drag coefficient (ΔC_d) was responsible for the increase in rotor lifted weight (ΔW) for a given power setting (C_p), a relationship between ΔC_d and ΔW was established and is shown in Figure 10. Using a linear regression technique, it was possible to establish a ($\Delta W / \Delta C_d$) ratio, which was valid and constant for a specific power setting. Multiplication of this ratio by the two-dimensional wing drag coefficient for each associated flap deflection angle made it possible to define a form of the rotor/wing download as:

$$DL = C_{D_{\delta_f}} \left[\frac{\Delta W}{\Delta C_D} \right] \Big|_{C_p} \quad (9)$$

Results of the experimental download analysis for the selected power setting ($C_p = .001$) were computed as percentages of the total aircraft thrust, which was a function of flap deflection angle. The computed download values are listed in Table 5 and depicted in Figure 11.

Table 5
Experimental Download

δ_f	W ($GW - 2F_j$)	DOWNLOAD $(\Delta W / \Delta C_d) C_{D_{\delta_f}}$	TOTAL THRUST ($W + DL$)	DOWNLOAD (% THRUST)
0	12402	1885	14287	13.2
20	12599	1706	14305	11.9
40	12753	1472	14225	10.3
50	12967	1249	14316	9.4
60	13079	1216	14294	8.5

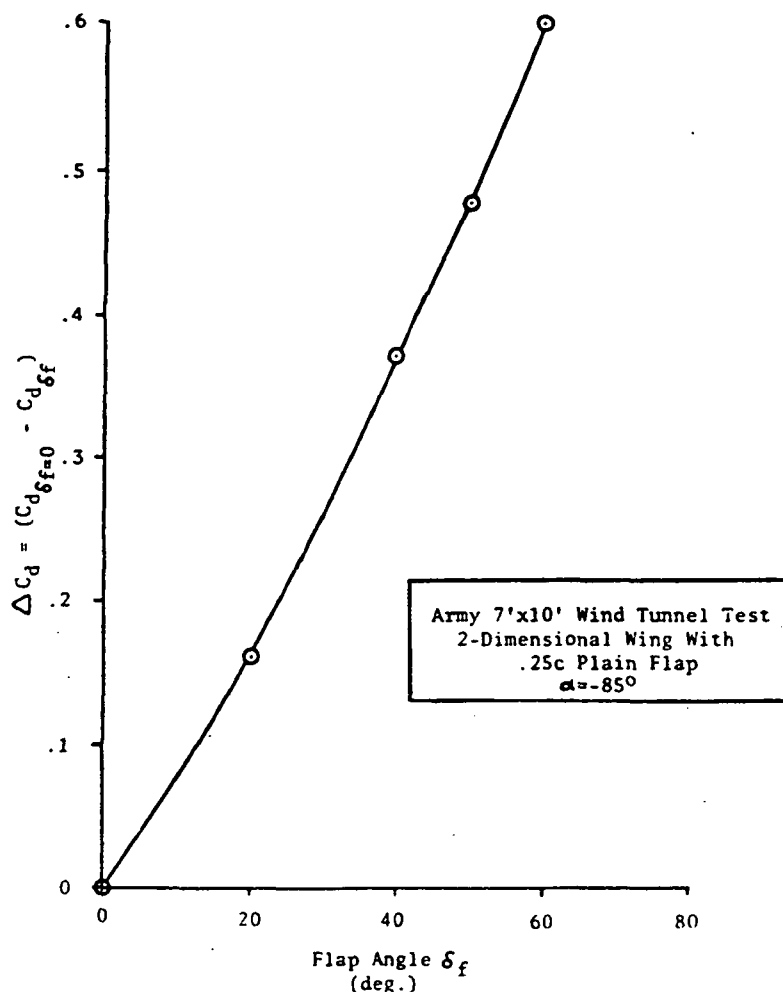


Figure 9

Effect of Flap Angle on Drag Coefficient Change, Referenced to the Drag Coefficient for 0° Flap Deflection

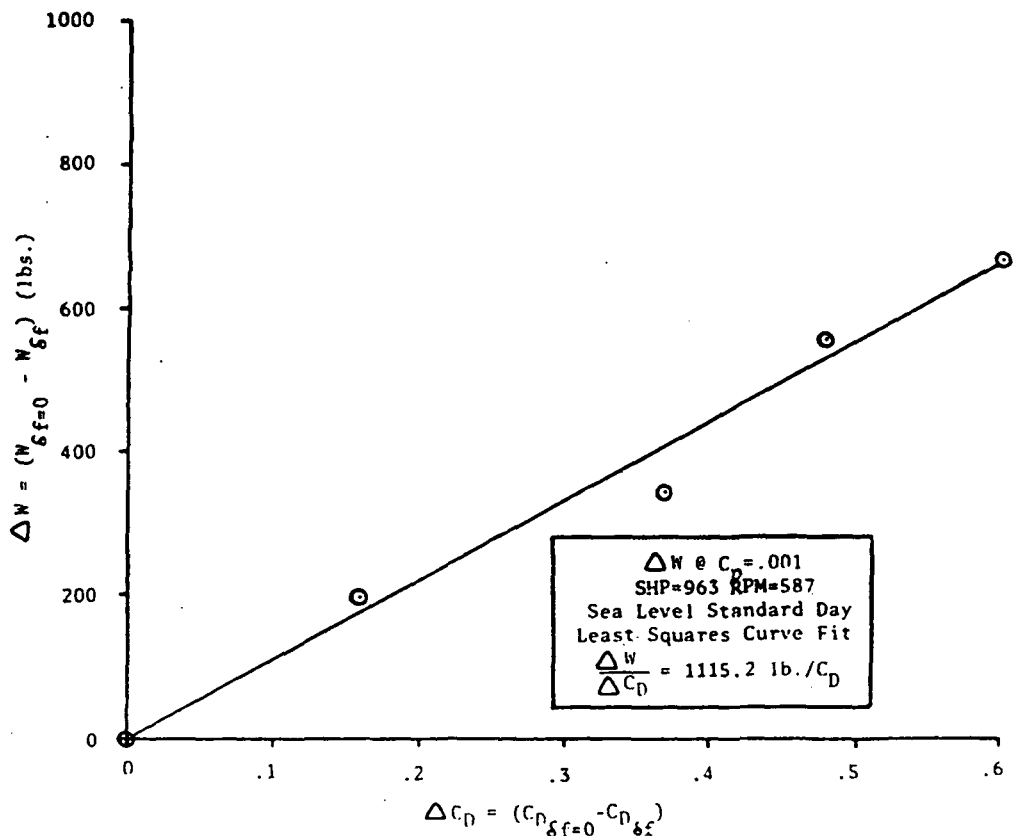


Figure 10

Change in Rotor Lifted Weight, Referenced
 to Rotor Lifted Weight for 0° Flap
 Deflection, as a Function of the
 Change in Drag Coefficient

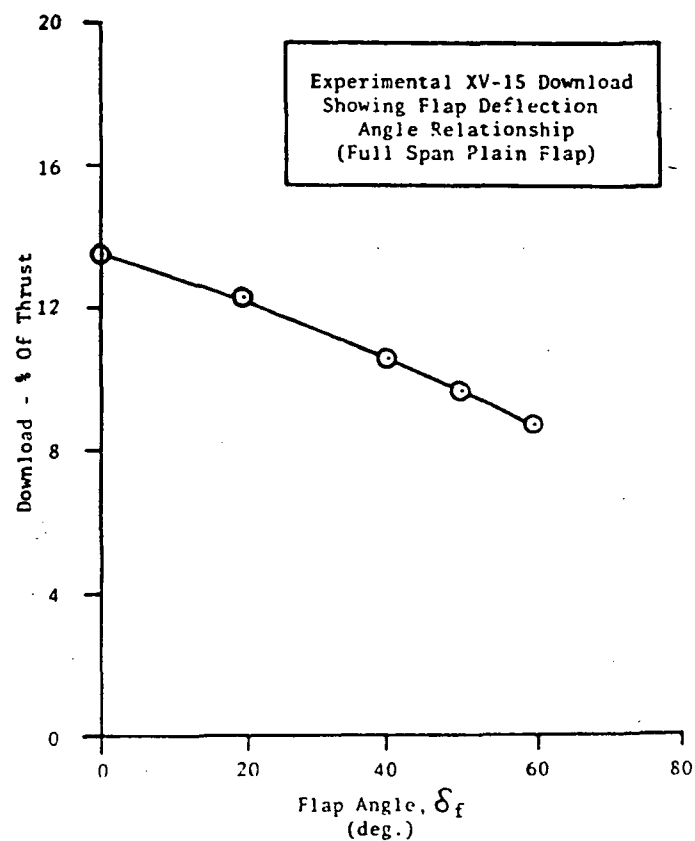


Figure 11

Experimental XV-15 Download As a Function
of Flap Deflection Angle

CHAPTER 3

Analytic Determination of the Download

The airflow from a spinning propeller, or prop-rotor in the present case, can be approximated through the use of vortex ring theory. A vortex ring is a vortex filament that forms a circle of radius r' . The approximation of the rotor's airflow in this study consisted of a set of concentric vortex rings, one set for each prop-rotor, beginning at a position that coincided with the geometric location of the rotor disks. This study was concerned with hovering performance simulation only, so the number of vortex rings to be included in the analysis was dictated by the hover scenario being analyzed, i.e., IGE or OGE.

The velocity of the air that impinges on the upper surface of the aircraft's wing is the cause of the rotor/wing download and hence was the parameter that needed to be determined. More specifically, the axial component of the rotor slipstream velocity needed to be determined.

Three aspects of the vortex system that required investigation in order for the analysis to be performed were: a set of equations that could be used to calculate the induced axial velocity components of each of a number of vortex rings; an equation that could model the rotor wake contraction, i.e., predict the radius (r') of each of the vortex rings downstream of the rotor disk; and a system

whereby spacing between each successive vortex ring could be adjusted to obtain an average induced axial velocity, at the rotor disk, that agreed with that predicted by momentum theory for helicopter rotor inflow.

Vortex Ring Induced Velocity

The velocity induced by a vortex ring can be determined by beginning with the Biot-Savart law written in vector notation:

$$\vec{dv} = \frac{r}{4\pi} \frac{\hat{R} \times \vec{ds}}{|\hat{R}|^3} \quad (10)$$

giving the velocity vector \vec{dv} induced by an element of length $ds = r'd\phi'$ of the vortex ring at the point (x, r, ϕ) or (x, y, z) (Figure 12). Forming the vector \vec{ds}/ds , which represents the unit vector tangent to the vortex ring at the position of the vortex element, with the unit vectors in the x , y and z directions gives:

$$\frac{\vec{ds}}{ds} = \hat{O}\hat{i} + \cos\phi'\hat{j} - \sin\phi'\hat{k} \quad (11)$$

Forming the radius vector \hat{R} , which represents the distance from the vortex element to the point (P) at which the induced velocity is to be calculated, in a similar fashion gives:

$$\hat{R} = x\hat{i} + (r\sin\phi - r'\sin\phi')\hat{j} + (r\cos\phi - r'\cos\phi')\hat{k} \quad (12)$$

with the magnitude of the vector being:

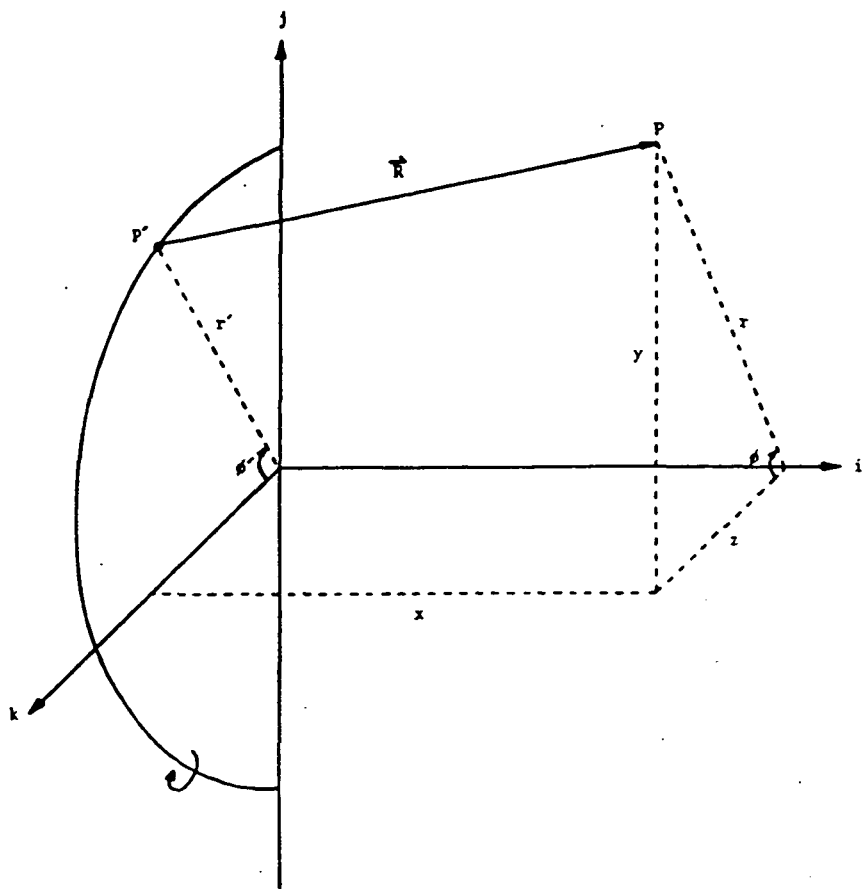


Figure 12

The Geometry Used for Deriving the Axial Velocity Component Due to a Vortex Ring

$$|\vec{R}| = \sqrt{x^2 + r^2 + r'^2 - 2rr'\cos(\phi - \phi')} \quad (13)$$

The cross product of the two vectors then becomes:

$$\vec{R} \times \frac{d\vec{s}}{ds} = -(r\cos(\phi - \phi') - r')\hat{i} + x\sin\phi'\hat{j} + x\cos\phi'\hat{k} \quad (14)$$

The x, or axial, component of the induced velocity caused by the whole vortex ring can then be determined by integrating the resulting Biot-Savart expression around the circumference of the ring. The expression to be integrated becomes:

$$v_{rx}(x, r) = -\frac{r}{4\pi r'} \int_0^{2\pi} \frac{r\cos(\phi - \phi') - 1}{[\sqrt{x^2 + r^2 + 1 - 2r\cos(\phi - \phi')}]^3} d\phi' \quad (15)$$

where the ratios x/r' and r/r' have been replaced by x and r for clarity. Following the steps outlined in Appendix C, the final form of the equation to be solved for the axial velocity component of the vortex ring is:

$$v_{rx}(x, r) = \frac{r}{2\pi r'} \left[\frac{1}{\sqrt{x^2 + (r+1)^2}} \right] \left\{ K(k) - \left[1 + \frac{2(r-1)}{x^2 + (r-1)^2} \right] E(k) \right\} \quad (16)$$

where $K(k)$ and $E(k)$ are those functions also shown in Appendix C. The axial velocity shows singular behavior at $x = 0$, $r = r' = 1$ and near this point the equation can be evaluated by expanding the elliptic integrals for $K(k)$ and $E(k)$ in powers of $(1 - k^2)$:

$$K(k) = \Lambda + (\Lambda - 1)/4(1-k^2) + (9/64)(\Lambda - 7/6)(1-k^2)^2 + \dots \dots \quad (17)$$

$$E(k) = 1 + 1/2(\Lambda - 1/2)(1-k^2) + (3/16)(\Lambda - 13/12)(1-k^2)^2 + \dots \dots \quad (18)$$

Where:

$$\Lambda = \ln \frac{4}{\sqrt{1 - k^2}} \quad k^2 = \frac{4r}{x^2 + (r+1)^2}$$

The remaining parameter that required attention in order to be able to evaluate the induced axial velocity equations was the vortex circulation strength, Γ .

Beginning with the Kutta-Joukowski law, which relates circulation to lift, or in this case thrust, an expression for circulation strength can be written:

$$\Gamma = \rho V_t r R \quad (19)$$

Utilizing the dimensionless thrust coefficient from standard helicopter terminology, the rotor-produced thrust can also be expressed as:

$$\Gamma = \rho A_D V_t^2 C_t \quad (20)$$

Equating these two expressions gives:

$$rR = A_D V_t C_t \quad (21)$$

or

$$\tau R = \pi R^2 V_t C_t \quad (22)$$

Differentiating both sides of this expression with respect to R gives:

$$\tau dR = 2\pi R V_t C_t dR \quad (23)$$

or

$$\tau = 2\pi R V_t C_t \quad (24)$$

This expression, while representing the circulation strength about a rotor disk of radius R , has also been shown to represent the total circulation strength about the axis of rotation due to the trailing vortex system (Franklin, 1955). Since this study involved a three-bladed prop-rotor system, it was assumed that the circulation strength due to each blade could be obtained by dividing the total circulation strength, about the axis of rotation, by three. Thus, the final form of the trailing vortex circulation strength due to each blade becomes:

$$\tau = \frac{2\pi R V_t C_t}{3} \quad (25)$$

Wake Contraction

A formula was needed that could be used to model the contraction of the rotor wake as a function of downstream

position from the rotor disk. From the literature investigated (Marr, Sambell, and Neal, 1973), a formula was obtained that, while not reflecting extreme precision, modeled the gross characteristics of the wake contraction. The expression is of the form

$$\frac{r(z)}{R} = 0.707 \left\{ \frac{1}{0.5[2 - e^{-nz/R}]} \right\}^{1/2} \quad (26)$$

where: $r(z)$ = downstream wake radius

R = rotor radius

z = downstream position

n = a constant

The determination of the constant, n , began with the continuity equation written between the rotor disk and a general point in the rotor wake. It can be shown, between these two points, that the following relation holds:

$$\frac{V_z}{V_D} = \left(\frac{R_D}{R_z} \right)^2 \quad (27)$$

Considering a velocity relationship of the form

$$\frac{V_z}{V_\infty} = \left[\frac{V_z}{V_D} \right] \left[\frac{V_D}{V_\infty} \right] \quad (28)$$

it can be written

$$\frac{V_z}{V_\infty} = \left(\frac{R_D}{R_z} \right)^2 \left[\frac{V_D}{V_\infty} \right] \quad (29)$$

This relationship was further developed by obtaining expressions for the ratios on the right-hand side. For the

velocity ratio it is accepted that the ratio of the inflow velocity at the rotor disk to that infinitely far downstream is 0.5. Marr, Sambell, and Neal (1973) theorized that the radius ratio R_z/R_d equals .908 at a value of z/R equal to 0.2. Substituting these values yielded a velocity ratio of

$$\frac{V_z}{V_\infty} = 0.60645 \quad (30)$$

Considering this relationship and that expressed by Equations (26) and (29), it can be shown that

$$\frac{1}{2} \left[2 - e^{-nz/R} \right] = 0.60645 \quad (31)$$

From which it follows that $n = 1.19706$.

Time Spacing of Vortex Rings

A method had to be devised whereby the spacing between vortex rings could be adjusted so that the average inflow velocity through the rotor disk, determined using the computer simulation model, could be made to agree with that predicted by the momentum theory for helicopter rotors (i.e., $v_i = v_t \sqrt{C_t/2}$).

Once again, beginning with the continuity equation, it is seen that

$$\frac{V(z)}{V_i} = \left[\frac{R_i}{R(z)} \right]^2 \quad (32)$$

Substituting Equation 26 for the radius ratio and squaring gives

$$\frac{V(z)}{v_1} = \left[2 - e^{-nz/R} \right] \quad (33)$$

Substituting the momentum theory for the induced velocity at the rotor disk gives

$$V(z) = v_t \sqrt{C_t/2} \left[2 - e^{-nz/R} \right] \quad (34)$$

Realizing that this represents velocity in the z direction, i.e., dz/dt , it can be rearranged to the form

$$\int_0^t dt = \frac{1}{v_t \sqrt{C_t/2}} \int_0^z \frac{dz}{\left[2 - e^{-nz/R} \right]} \quad (35)$$

Integration of this equation yields the final form as

$$Kt = \frac{1}{v_t \sqrt{C_t/2}} \left[\frac{z}{2} + \frac{R}{2n} \log \left(2 - e^{-nz/R} \right) \right] \quad (36)$$

The constant, K, was introduced to provide the means for time spacing adjustment of the vortex ring elements, as stated earlier.

Analytic Download Analysis

With all the components identified and accounted for, the task of modeling the XV-15 propulsion system flow, for the purpose of analytically approximating the aircraft download, could be begun.

Due to the dependence of the time equation (Equation 36) and the velocity equation (Equation 16) itself on the rotor tip speed, a constant tip speed had to be established. The actual aircraft hovers at 98% of the full rotor speed of 601 RPM, or 588.98 RPM. This rotor speed corresponds to a tip speed of 768.38 ft/sec and, since it represents the actual hover condition, was the constant tip speed chosen. At this speed each rotor blade completes one revolution approximately every .1022 seconds. The vortex system that is actually generated by the rotor resembles three continuous shed vortices that together form a contracting helicoil shape proceeding downstream from the rotor disk. It was assumed, for this study, that the actual vortex system could be adequately modeled by breaking the three concentric helical vortices into three concentric vortex rings. In this scheme, three vortex rings were considered shed for each rotor revolution, one for each rotor blade. It was initially assumed that the vortex rings would be equally spaced over the time it took the rotor to complete one revolution (i.e., a vortex ring was assumed to be shed from the rotor approximately every .034 seconds). Because Equation 36 could not be solved explicitly for downstream position of the vortex rings as a function of time, another procedure was implemented. Because the entire analysis was performed for three thrust coefficients, Equation 36 was plotted using each thrust coefficient and whole values of z , the downstream position

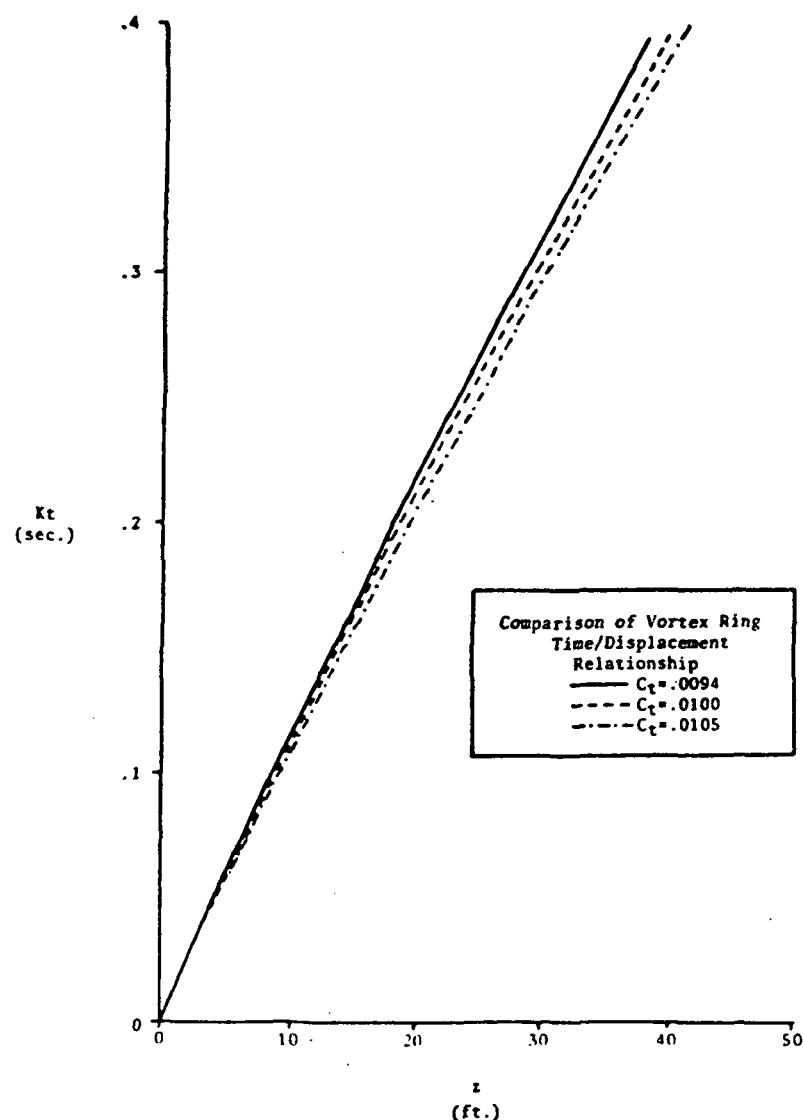


Figure 13
**Vortex Ring Downstream Position as a
Function of Time**

of the vortex rings (Figure 13). Then, using five sets of points from each resulting curve, a fifth order interpolating polynomial was formed for each thrust coefficient dependent curve. This resulted in three fifth order polynomials that were explicitly solvable for the vortex ring downstream position as a function of ring time spacing. Up to this point the time spacing factor, K, had been held constant at unity and was retained in the interpolating polynomials. Then, beginning with the initial time spacing of the vortex rings (.034 seconds between rings), the downstream distance that each ring had been displaced from the rotor disk could be calculated. With this distance known, the associated vortex ring radii could be calculated (Equation 26) and the contribution of each ring to the total axial velocity at the points of consideration could be computed. The ring spacing factor K could then be adjusted and the computations performed again until successive iterations arrived at the desired result.

Computer Program Calibration

The average inflow velocity at the rotor disk dictated by simple momentum theory is dependent on both tip speed and thrust coefficient. Hence, the calibration of the spacing factor K had to be performed for each of the three different thrust coefficient cases.

The geometry of the calibration program was set up in such a manner that the points at which the velocities were calculated coincided with the aircraft's rotor plane. The

calculations were begun 2.5 feet outboard of the rotor tip path and proceeded in one-foot increments through the rotor plane to a point 2.5 feet outboard of the rotor tip path on the opposite side. For each point the axial velocity component due to each of the vortex rings was calculated. These components were then summed to arrive at a total axial velocity for each point. Because the aircraft rotors are 25 feet in diameter, this scheme led to a total axial velocity value for each of 31 points. The 25 velocity values that occurred in the "rotor disk" were then averaged to arrive at an average inflow velocity through the rotor disk. The vortex ring spacing factor K was then varied until the average inflow velocity through the rotor disk agreed with that predicted by momentum theory. Small K values packed the rings more closely and resulted in higher average velocities, while large K values spaced the rings out and resulted in lower average velocities. The range of K was between zero and one. The K values that resulted in the correct average inflow velocities were then retained and used later in the version of the program that computed aircraft download.

The number of vortex rings in the calibration program analysis was limited to 72. This number of rings produced adequate results evidenced by the fact that increasing the number of rings included in the analysis to 100 increased the average inflow velocity through the rotor disk by a maximum of .39%.

Download Computer Program

With the proper predetermined spacing factor K, the program version that calculated the analytic download could be formulated.

The geometry of the analysis consisted of two systems of vortex rings, each concentric, their centerlines separated by approximately 32 feet. The axial velocities were calculated at 71 points; beginning at a point approximately 6.5 feet outboard of one rotor tip path and progressing, in one-foot increments, to a point approximately 6.5 feet outboard of the other rotor tip path. The points at which the velocities were calculated were 4.67 feet below the rotor planes, coinciding with the position of the wing on the aircraft itself.

Both IGE and OGE hover scenarios were investigated. For the OGE scenarios ($H/D = \text{infinity}$), each rotor was modeled by 72 concentric vortex rings for a total of 144 rings. For the IGE scenarios ($H/D = 2.0, 1.0$ and 0.5), the number of vortex rings used was dictated by the H/D ratio. For these cases the corresponding rotor heights were 50, 25 and 12.5 feet, respectively. The ground plane was modeled by using a mirror image of the shed vortex system, reflected about the "ground plane." This was accomplished in the following manner. The H/D ratio to be investigated was a program-prompted input. If it was an IGE hover condition, this input set the required distance that separated the rotor plane from the ground plane. Then, while

going through the program loop that calculated the vortex rings' downstream positions, the positions were monitored until a position was reached that corresponded to the required distance between the rotor and ground plane. At this point, the next vortex ring that was formed was identical to the one that occurred at the ground plane position and in fact was superimposed on the ring that occurred at the ground plane. The next ring that was formed was identical to the ring that preceded the ring that occurred before the ground plane position. Each successive ring that was formed for the reflected ring system was identical to its corresponding ring in the shed vortex system (Figure 14). The circulation strengths on the superimposed mirror image system, however, were reversed. With all the positions and radii of the vortex rings determined, the total axial velocity at each point of concern could be computed. The velocities from successive points were then averaged and used to form an average dynamic pressure, q , based on standard sea level conditions.

Values for the wing drag coefficients were taken from wind tunnel tests of a representative, two-dimensional wing section. The wing section was equipped with movable flaps that permitted testing at deflections of 0° , 20° , 40° , 45° , and 60° . The wing section was tested at angles of attack near -90° . The results of these tests provided five different drag coefficients corresponding to the five flap angle

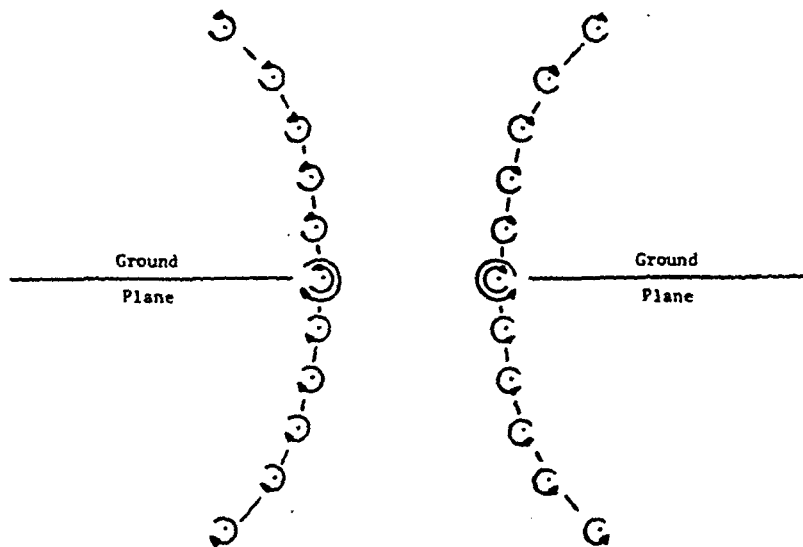


Figure 14

In Ground Effect Vortex Ring Representation

deflections. The flap deflection angle to be analyzed was a program-prompted input.

With the averaged dynamic pressures and drag coefficients determined, all that remained to be done, for download or drag considerations, was to determine an appropriate surface area. Due to the fact that the points used to arrive at the averaged dynamic pressure were separated by one foot, this one-foot length was multiplied by 5.25 feet, the aircraft wing chord. This 5.25-square-foot area was used between the vortex system centerlines, as the rotors are positioned on the wing tips of the aircraft. Each averaged dynamic pressure was then multiplied by a 5.25-square-foot-area and the appropriate drag coefficient, depending on the flap deflection angle, to arrive at a

component of drag or download. The drag components across the wing were then summed to arrive at a total value of drag. The resulting total drag or download value was then divided by the total rotor-produced thrust, determined by the thrust coefficient being investigated. This gave results for download as a percentage of total aircraft thrust. Listings of both the calibration and download versions of the XV-15 program are included in Appendixes D and E.

Velocity Profiles

During the formulation of the propulsion system computer simulation program, it was necessary to check each of the velocity components against published values (Deckert and Ferry, 1960) before the total velocities were computed. This was done in order to check the accuracy of the values from the computer program. The published values are presented as numbers that are dependent on the rotor radius to vortex ring radius (r/r') ratio and also on the distance between the point at which the velocity is being calculated and the vortex ring centerline to vortex ring radius (x/r') ratio. The published numbers are then multiplied by two π , the vortex ring radius (r') and divided by the circulation strength to arrive at the velocity value. Manually calculating these two ratios and knowing the circulation strength permitted a spot check of some of the number of velocity components that resulted from the computer program against the published values. When these values agreed, it

was concluded that the program was functioning correctly and the correct total velocity at each point would result.

An interesting intermediate result was obtained when the program was next set up to calculate the total axial velocity at each point along the line between the two rotor centerlines. These results produced a two-dimensional cross section of what was theoretically occurring to the rotor airflow due to the proximity of the rotors and the geometry of the installation. The resultant total axial velocities were bilaterally symmetric and are presented for each of the three thrust coefficients in Figures 15, 16, and 17.

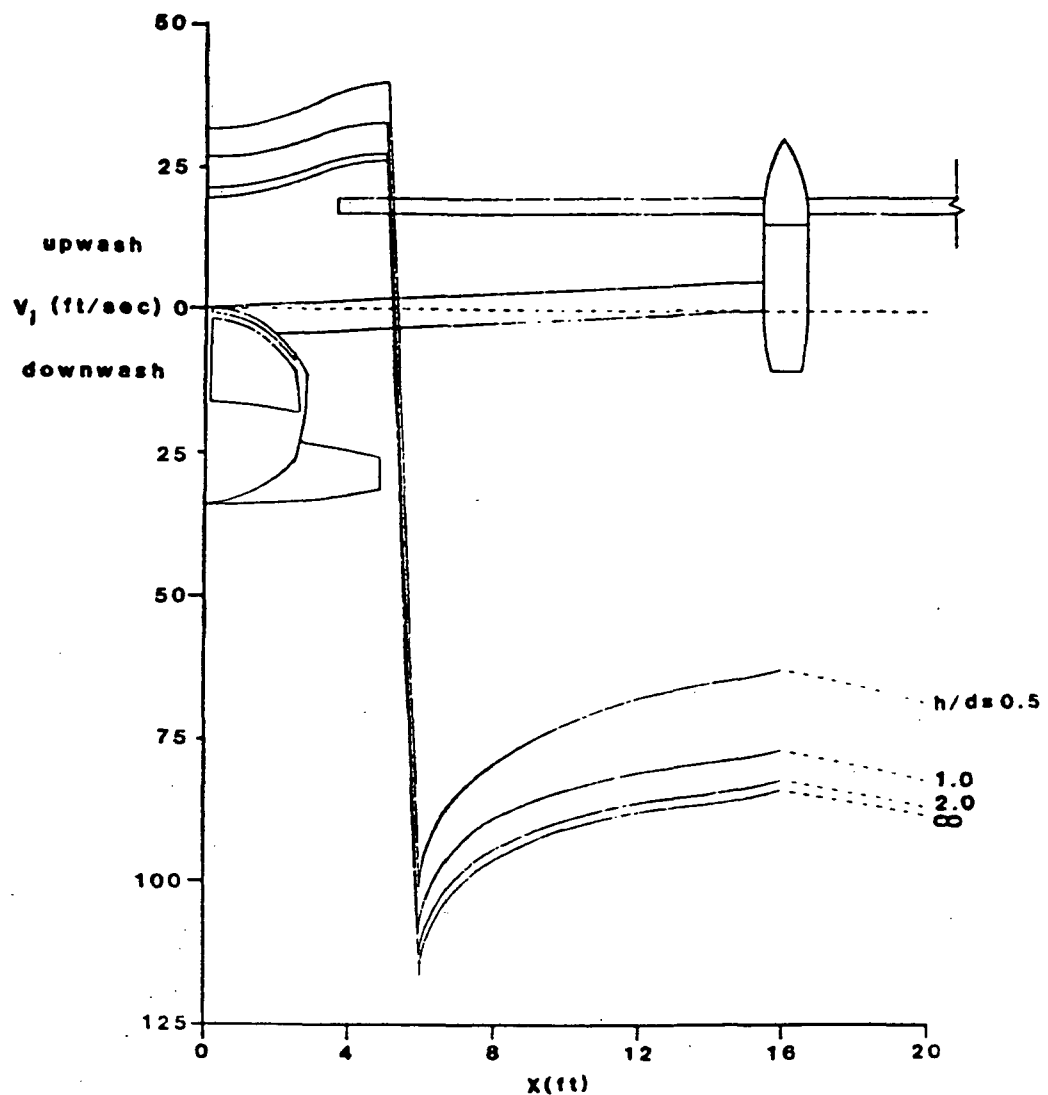


Figure 15

Computer-Generated Velocity Profile,
 $C_t = .0094$

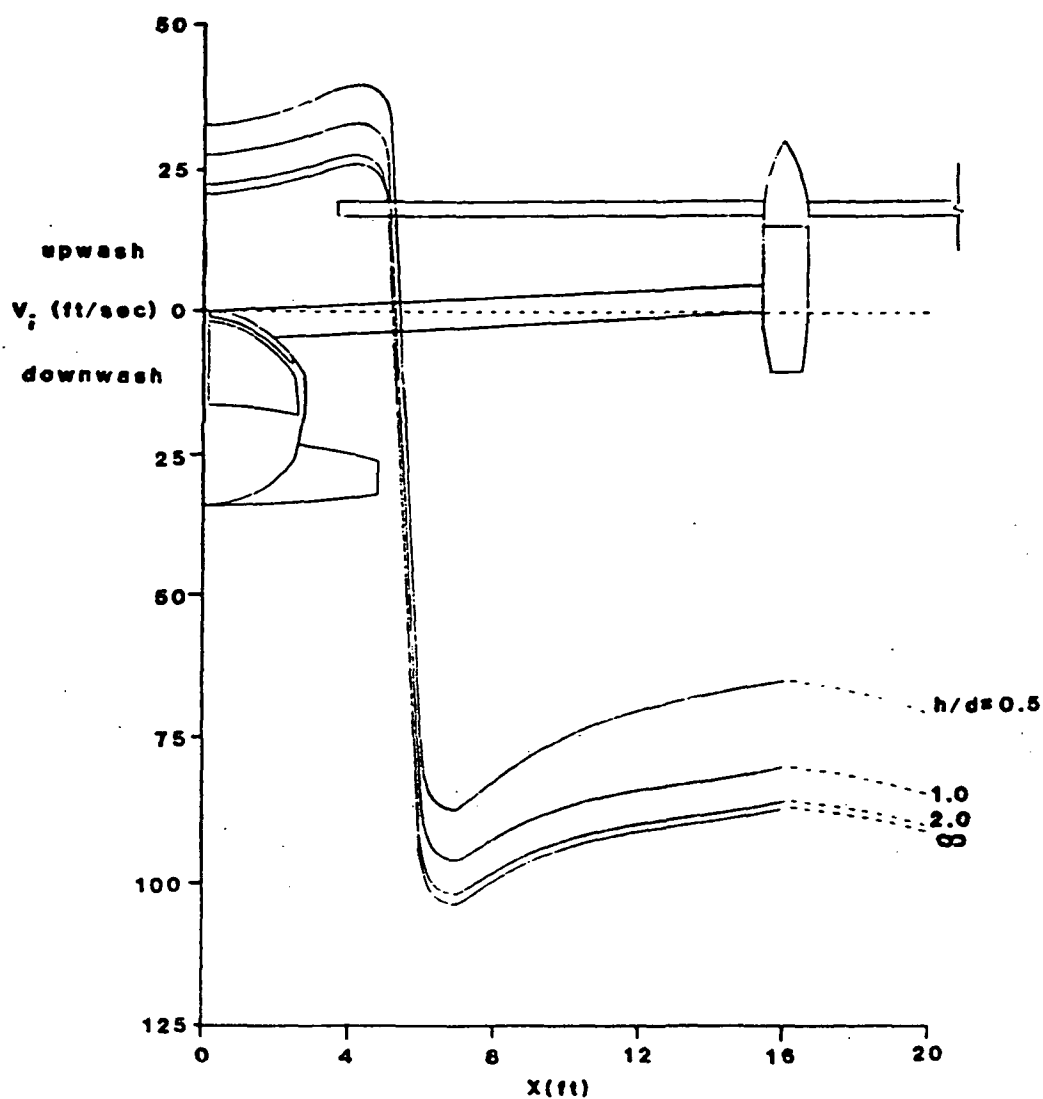


Figure 16

Computer-Generated Velocity Profile,
 $C_t = .01$

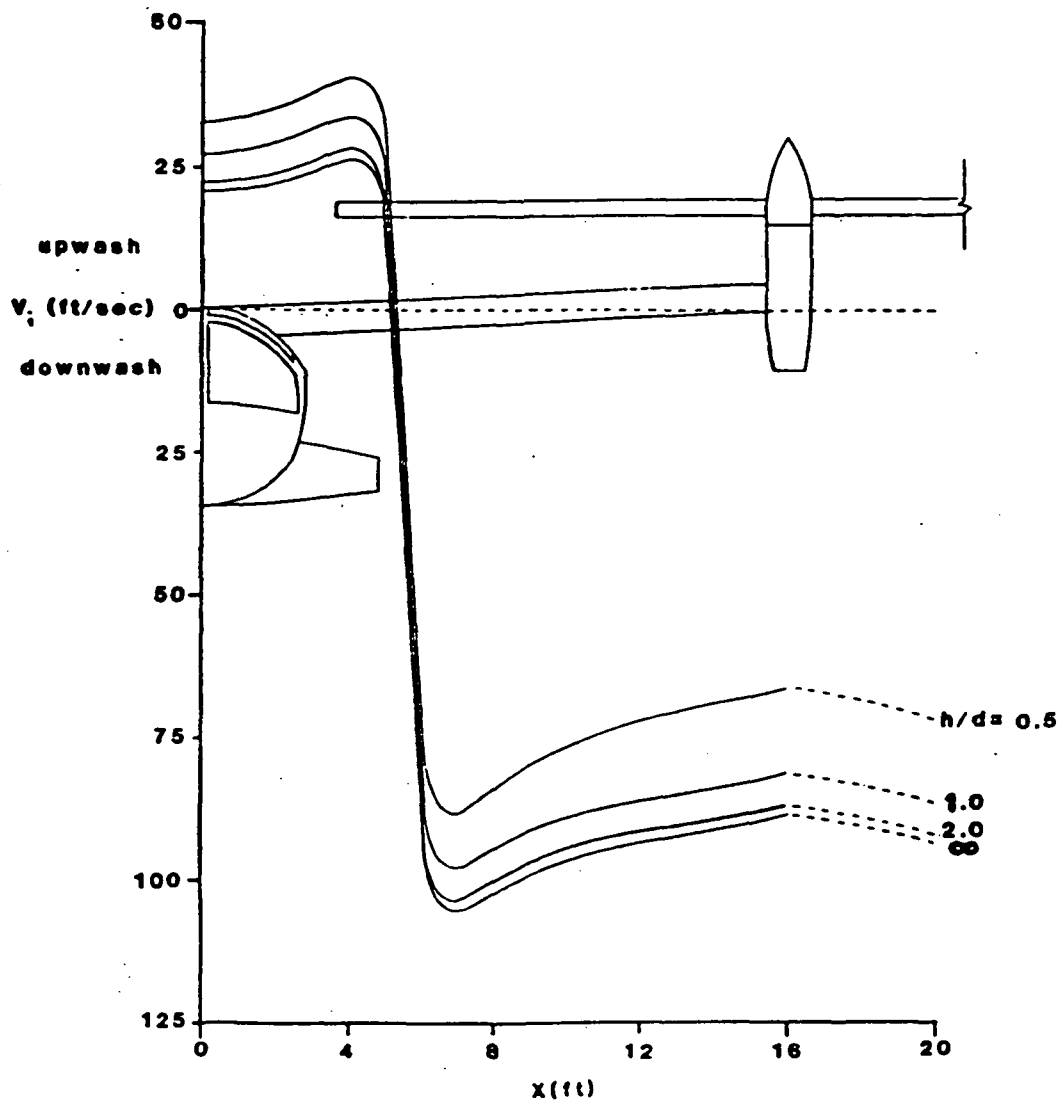


Figure 17

Computer-Generated Velocity Profile,
 $C_t = .0105$

CHAPTER 4

Model Test

After it was determined that the velocity values from the computer program were accurate, it was desirable to formulate a test for the download aspect of the program to demonstrate its validity. This was accomplished by using a model rotor system, a schematic of which is presented in Figure 18.

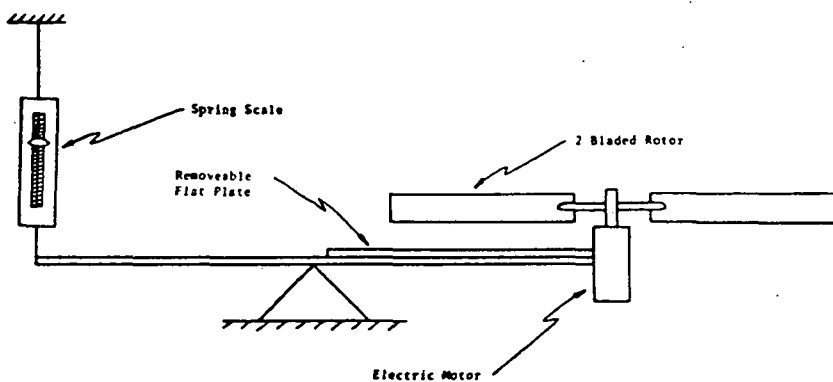


Figure 18
Model Rotor Test Setup

The model consisted of a 1.135-foot radius, fixed collective pitch rotor. The rotor had no provisions for cyclic pitch. The rotor was powered by a small DC motor that was powered by an instrumented power source. Power was transferred from the motor to the rotor by a shaft and

gear system. The power that was input to the motor was monitored through the use of volt and ampere meters on the power source. The thrust output by the rotor was determined through the use of a spring scale mounted at the opposite end of a statically balanced lever arm.

The model rotor system was operable both with and without a flat plate "wing" section placed 1.5 inches below the rotor disk. It was thought that by operating the model system both with and without the wing installed, monitoring the power source, spring balance and rotor RPM, the download on the flat plate "wing" could be deduced.

A computer program was formulated to simulate the model performance. Both the calibration and download versions of the model program are included in Appendixes F and G. These programs were constructed in exactly the same manner as were the programs that modeled the XV-15.

CHAPTER 5

Results and Discussion

Experimental Download Analysis

Values of rotor/wing download for the XV-15 Tilt Rotor Research Aircraft were deduced by combining the results from actual aircraft hover tests and wind tunnel tests of a representative two-dimensional wing section.

The hover tests were conducted at NASA Ames Research Center in 1983. The aircraft was modified to allow the flap and flaperon control surfaces to operate as one. This provided the effect of a full span plain flap system. The aircraft gross weight was closely monitored and maintained within a 200-pound range. The rotor speed was held constant during the hover test points.

The wind tunnel tests were also conducted at Ames Research Center, but in the Army 7-foot by 10-foot wind tunnel. These tests resulted in drag coefficients for an airfoil section that had a .25c operable flap and was tested at angles of attack near -90°.

The values of the rotor/wing download that resulted from combining the data of these two tests are tabulated in Table 5 (page 24) and presented graphically in Figure 11 (page 27). The values determined for the download phenomenon ranged from 13.2% of total aircraft thrust (DL/T) for a 0° flap deflection to 8.5% (DL/T) for a 60° flap

deflection, both at a power coefficient (C_p) equal to .001. While these results appear reasonable, they are larger than those previously predicted for the XV-15 download phenomenon. Investigation of past studies that analyzed the download phenomenon, however, revealed that the magnitude of the resulting download values has increased. Thus the larger values produced by this study agree with the trend. However, there are some aspects of the experimental analysis that merit investigation.

The XV-15 was not flown in its regular configuration for the hover tests used for this study. A special modification was made to the flap/flaperon system so they could be deflected as one control surface. Thus, the data taken for this study reflect an XV-15 aircraft with a full span plain flap instead of the actual flap/flaperon system. While some data exist that reflect the actual flap/flaperon system, the limited number of test points and data scatter prevent a comparison to the full span plain flap data. Hence, as a result of this study, it can be deduced that the actual download for the XV-15, in the nominal hover configuration (40° flap/ 25° flaperon) lies between the 25° full span plain flap value of 11.5% DL/T and the 40° full span plain flap value of 10.4% DL/T. Hence, more OGE hover tests of the XV-15 with the "as-built" flap/flaperon system, at various angles of deflection, are required to narrow this download range and better define the XV-15 download.

The wind tunnel tests of the two-dimensional wing section, while providing valid results for the "as tested" configuration, did not adequately model the actual flow field in the vicinity of the aircraft. Since the tests have been completed, more understanding has been developed about the flow field that exists about the XV-15. A region exists, midway between the rotor centerlines, where there actually is an "upwash." This is caused by the radial components of the rotor wakes that travel along the wing span and intersect in the vicinity of the aircraft centerline, turning upward. This flow phenomenon was validated in the subsequent computer simulation model of the XV-15 done for this study. The existence of this upwash is documented in the velocity profile plots (Figures 15, 16, and 17). Due to this fact, and another more obvious limitation, the extension of the two-dimensional drag data to adequately represent the aircraft wing drag is questionable. The more obvious limitation is encountered in the process of transforming two-dimensional airfoil section data to reflect three-dimensional characteristics. While the transformation of sectional data to reflect wings of finite aspect ratio is, in general, easily accomplished, it is not so in this case. A better representation of the airflow about the wing of the XV-15 must be established in order to obtain more closely representative drag data. It is believed that tests must be performed with a wing, instrumented to obtain force and moment data, placed

downstream and in between two contra-rotating prop-rotors. Whether this test is run with scale-model or actual-size hardware, it would further the understanding of the wing drag characteristics as they apply to the XV-15 configuration.

The assumption that the download-to-thrust (DL/T) ratio was a constant for a given flap angle deflection was found to be accurate when applied to a constant C_p analysis. The download-to-thrust ratio was found to actually increase slightly with increasing power coefficient, but this increase amounted to only 2% over a range of C_p from .0006 to .0015.

A method that more accurately predicts the engine exhaust jet thrust must be developed. The method used for this study relied on the assumption that the average inflow velocity, as predicted by simple momentum theory, adequately represented the velocity in the vicinity of the engine inlet. To better understand the engine inflow velocity, pressure surveys of that area should be performed. The magnitude of the exhaust thrust, however, was small enough that its contribution to the analysis was minor.

The correction of the power polar (C_p vs. $C_t^{3/2}$) algorithm to reflect the nonlinear aerodynamic effects at high C_p values also deserves more study and validation.

Model Test Analysis

The model test and subsequent computer simulation of the model did not supply results with the desired precision. The results that were produced, however, compare favorably. The model test resulted in a download-to-thrust (DL/T) ratio of 11.2% of rotor thrust at a thrust coefficient of .0075 and an H/D ratio of infinity. The computer simulation of the model, however, produced a DL/T ratio of approximately 9.7% for the same conditions. The difference (approximately 13%) between the two values could be attributable to a few factors.

First is the validity of taking two-dimensional drag data and applying it to a three-dimensional test. The drag coefficient for the computer simulation was taken to be 1.98 based on the literature reviewed (McVeigh, 1985). This represented a flat plate oriented perpendicular to the flow (i.e., an angle of attack of -90°), tested at Reynold's numbers between 10,000 and 1,000,000. Since there were no provisions on the model setup to measure the velocities that occurred at the wing surface, a determination of the test Reynold's number was not possible. It is also thought that a better understanding of the drag characteristics should be obtained. This would allow the computer program to model more precisely the actual test conditions. A model system should be built and tested that incorporates a wing, instrumented to provide force and moment data, separate from the rotor force system. This would allow direct

measurements and correlation of the download force on the wing and the rotor-produced thrust.

While some of the aspects of the model test could benefit from further refinement, the test provided an interesting result. The comparison between the model test and computer simulation did show, in this case, that the computer simulation provided a lower estimate of the download than did the model test. This provided the valuable information that the computer simulation predicts lower download values than those which actually occur. Extended to the aircraft simulation program, this means that the magnitude of the actual download is at least as large as the analytically determined download.

Analytic Download Analysis

This aspect of the study was developed with contributions from a number of sources. The main component of the study was the theory involved in modeling an aircraft rotor system's airflow through the use of vortex ring theory.

Formulas were developed that modeled the rotor wake contraction downstream of the rotor disk (Equation 26) and also allowed for adjustment of the time spacing of the vortex rings in the wake (Equation 36). A formula was also obtained that allowed determination of the needed vortex ring circulation strength (Equation 25). Then, beginning with the Biot-Savart law, a formula was developed that permitted calculation of the axial velocity component due to each of the vortex rings (Equation 36). The velocity

components were then summed and used in conjunction with the aforementioned wind tunnel drag coefficients to arrive at download values. This analysis was performed for three different thrust coefficients and four H/D ratios for each thrust coefficient. These download values are tabulated in Table 6. Figure 19 is presented to show the effect that different H/D ratios had at a constant thrust coefficient of .0094 on the theoretical download values. The effects that different thrust coefficients had on the download results were too small to allow an adequate graphic comparison. The range of download values for this method of analysis varied from 14.44% DL/T for a 0° flap deflection to 9.233% DL/T for a 60° flap deflection, both at H/D equal to infinity and C_t equal to .0105. Changing the H/D ratios from infinity to 0.5 had the effect of reducing the DL/T ratio by from 5% to 7%. There are, however, a few aspects of this method of analysis that warrant further investigation.

The method by which the circulation strength of the vortex rings was determined requires further investigation and refinement. The velocity components that were computed using this method are directly proportional to the circulation strength, hence the circulation strength is an important parameter. While the method presented seems rational, it is thought that other factors that were not investigated could affect the circulation strength. One such aspect is the assumption that the circulation strength

Table 6
Analytic Download

C_t	h/D	$\frac{D}{T} \mid_{\delta_f=0^\circ}$ (%)	$\frac{D}{T} \mid_{\delta_f=20^\circ}$ (%)	$\frac{D}{T} \mid_{\delta_f=40^\circ}$ (%)	$\frac{D}{T} \mid_{\delta_f=45^\circ}$ (%)	$\frac{D}{T} \mid_{\delta_f=60^\circ}$ (%)
.0094	0.0	14.429	12.919	11.241	10.737	9.227
	2.0	13.848	12.403	10.797	10.315	8.869
	1.0	11.919	10.691	9.325	8.916	7.687
	0.5	7.368	6.632	5.814	5.569	4.833
.01	0.0	14.424	12.914	11.236	10.733	9.223
	2.0	13.807	12.366	10.765	10.285	8.844
	1.0	11.717	10.511	9.170	8.768	7.562
	0.5	7.567	6.811	5.970	5.718	4.961
.0105	0.0	14.440	12.928	11.248	10.744	9.233
	2.0	13.784	12.345	10.747	10.268	8.829
	1.0	11.794	10.579	9.229	8.824	7.609
	0.5	6.625	5.967	5.236	5.017	4.360

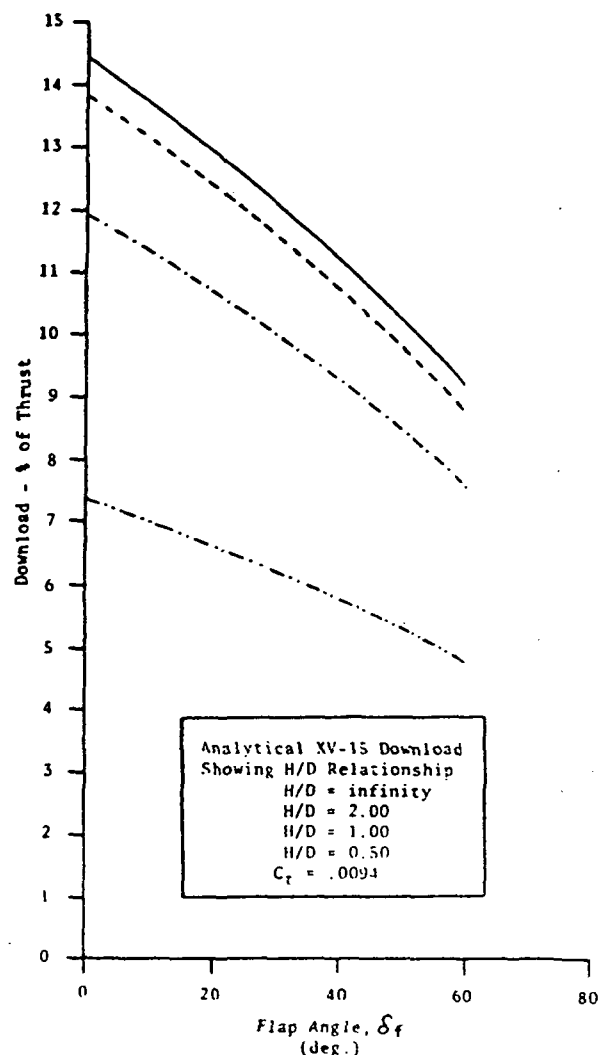


Figure 19
Effect of Hover Height on Analytic XV-15 Download

remains constant in the vortex ring as it translates down the rotor wake, while it is believed that a decay of circulation strength actually occurs. In order to better resolve this issue, rotor tests that address the circulation strength phenomenon should be performed.

The formula (Equation 26) that models the rotor's wake contraction as a function of downstream distance from the rotor disk also requires more investigation. Analytical methods have been produced since Equation 26 was developed in 1982 that more closely model the actual behavior of the wake downstream of the rotor disk. These methods should be incorporated into this type of computer simulation analysis to reflect the increased knowledge of rotor wake contraction. The constant, n, in Equation 26 should be investigated further to determine its control of the final wake shape and overall characteristics. It is thought that a better method of solving for this constant could be devised and implemented in the analysis.

The fact that this computer simulation concerned itself with only the airflow due to the two aircraft rotors and not any of the contributions due to the body effects of the aircraft itself sheds some doubt on the precision of the final answers. While the resulting values of download are reasonable, the inclusion of the aircraft body into the analysis would no doubt have an effect on the final results. For further study, the results of this analysis could be used in conjunction with a method that included

the physical body of the aircraft to better understand the wake/body characteristics that contribute to the download phenomenon. This could also be extended to gain a better understanding of the sensitivity of the download to basic configuration changes of the aircraft body shape.

While extension of the wind tunnel data to reflect the actual aircraft conditions is suspect, in the case of the computer simulation it is thought that the wind tunnel results adequately represent the situation that exists in the computer simulation. The computer simulation concerned itself with only the determination of the axial components of the velocity that exist on the upper wing surface. Since the wind tunnel tests essentially reflected only axial and not radial velocities, i.e., spanwise flow, it is thought that the results from the wind tunnel tests and computer simulation were compatible. Hence, the results from both tests, when combined, were thought to form a valid analysis procedure. Further tests should be performed to either validate this assumption or develop a more nearly correct means of representation of the flow characteristics.

The intermediate results of the velocity profiles demonstrated the validity of the upwash phenomenon that occurs between the rotors along the aircraft centerline. This upwash has since been further validated through the use of flow visualization techniques applied to both the aircraft itself and model tests. The inclusion of this

phenomenon in the download picture presents another factor to be considered.

CHAPTER 6

Conclusion

Analysis of the download phenomenon, which occurs when the XV-15 Tilt Rotor Research Aircraft is flying in the hover/helicopter configuration, was pursued utilizing two different methods. The download is a result of the aircraft's wing being in close proximity (approximately 5 feet) and parallel to the two rotor disks. The download force has the direct effect of reducing the aircraft's useful hover load and hence is an important parameter when considering tilt rotor aircraft.

The first analysis method utilized results from actual aircraft hover tests and wind tunnel tests of an XV-15 representative wing section. The download results for this method ranged from 13.2% DL/T for a 0° flap deflection to 8.5% DL/T for a 60° flap deflection, both at an H/D of infinity and a C_p of .001.

The second analysis method relied on an analytical model of the aircraft's two prop-rotors and their associated airflow. The model was then used to determine the axial velocities that occur at the position which the aircraft wing occupies. By then applying the drag coefficients from the aforementioned wind tunnel tests, download values resulted. A computer program was utilized for this analysis method. The results for this analysis method

ranged from 14.44% DL/T for a 0° flap deflection to 9.233% DL/T for a 60° flap deflection, both at an H/D of infinity and a C_t equal to .0105. The analytical analysis was performed for each of three thrust coefficients (.0094, .01, .0105) and also included the investigation of four H/D (infinity, 2.0, 1.0, 0.5) ratios for each thrust coefficient. The effect that the different H/D ratios had on the download results was quite apparent. Reducing the H/D ratio from infinity to 0.5 had the effect of reducing the DL/T ratio by from 5% to 7%. However, the effect that the different thrust coefficients had was not pronounced enough to allow any conclusion to be drawn.

A model rotor system was tested and analytically modeled in an attempt to validate the computer analysis. While the results did not agree with the desired precision, reflecting a 13% difference, the download results of the computer analysis were lower than those of the model test. This implied that the computer program predictions were within the lower bounds of the actual aircraft download values.

This study does not represent the definitive download analysis. At the time that this report was written, there were at least two other separate studies being conducted in attempts to better define the XV-15 download issue. One study is utilizing a powered model of the XV-15 aircraft with wing surfaces instrumented to obtain force and moment data. An additional objective of this test is to

investigate flow control, i.e., suction and blowing, and its ability to lessen the model download forces. Another study, utilizing the XV-15 aircraft, is attempting to establish a relationship between rotor thrust and hub spindle beam bending moments to resolve the download issue. It is thought that if this relationship can be established from data taken with the aircraft on the tie-down stand at NASA Ames Research Center, it can be applied to data recorded in free hover flight and download values will be determinable.

The download phenomenon is an extremely important performance parameter for the tilt rotor family of aircraft. When viewed in a useful load context, the download can be responsible for large reductions in the aircraft hover weight capabilities. With the V-22 aircraft coming into production for military and even possibly civil applications, more effort must be made to better understand and define the download phenomenon. It is only when a problem is fully understood and defined that intelligent attempts to deal with it are possible.

References

- Deckert, Wallace H.; and Ferry, Robert G. "Limited Flight Evaluation of the XV-3 Aircraft." Air Force Flight Test Center, Edwards AFB, CA, 1960.
- Dommasch, Daniel O. Elements of Propeller and Helicopter Aerodynamics. New York: Pitman, 1953.
- Franklin, Philip. A Treatise on Advanced Calculus, 5th printing. New York: John Wiley and Sons, 1955.
- Gillmore, K. B. "Survey of Tilt-Rotor Technology Development," presented at AGARD Flight Mechanics Panel Meeting on Advanced Rotorcraft, NASA Langley RC, 1971.
- Gessow, Alfred; and Myers, Garry C. Jr. Aerodynamics of the Helicopter, 6th printing. New York: Frederick Ungar, 1952.
- Hayden, James S. "The Effect of the Ground on Helicopter Hovering Power Required." United States Army Aviation Engineering Flight Activity, 1976.
- Hoerner, Sighard F. Fluid Dynamic Drag, 2nd ed. Great Britain: Published by the author, 1965.
- Jahnke, Eugene; and Emde, Fritz. Tables of Functions With Formulae and Curves, 4th ed. New York: Dover, 1945.
- Kuchemann, Dietrich; and Weber, Johanna. Aerodynamics of Propulsion, 1st ed. New York: McGraw-Hill, 1953.
- Magee, John P. "Download Estimation for JVX Technical Evaluation of Tilt-Rotor Configuration." Unpublished notes, 1982.
- "Tilt-Rotor Technology Thrusts." Society of Automotive Engineers Technical Paper Series, October 1983.
- Maisel, M.; and Harris, D. "Hover Tests of the XV-15 Tilt-Rotor Research Aircraft." American Institute of Aeronautics and Astronautics, AIAA-81-2501, 1981.

Makofski, Robert A.; and Menkick, George F. "Investigation of Vertical Drag and Periodic Airloads Acting on Flat Panels in a Rotor Slipstream." NACA Technical Note, TN 3900, 1956.

Marr, R. C.; Sambell, K. W.; and Neal, G. T. "V/STOL Tilt-Rotor Study, Volume VI, Hover, Low Speed and Conversion Tests of a Tilt-Rotor Aeroelastic Model." Bell Helicopter Company Final Report No. 301-099-002, May 1973.

McVeigh, Michael A. "V-22 Tilt-Rotor Large Scale Rotor Performance/Wing Download Test and Comparison With Theory." 11th European Rotorcraft Forum, September 1985.

Appendix A

Transformation from Equation 6 to Equation 7

$$\begin{aligned}
 1 + \frac{DL}{W} &= \frac{W+DL}{W} \\
 &= \frac{1}{\frac{W}{W+DL}} \\
 &= \frac{1}{\frac{W+DL-DL}{W+DL}} \\
 &= \frac{1}{1 - \frac{DL}{W+DL}}
 \end{aligned}$$

But from equation 5a -

$$T = W + DL$$

so -

$$1 + \frac{DL}{W} = \frac{1}{1 - \frac{DL}{T}}$$

and -

$$1 + \frac{DL}{W} = \left(1 - \frac{DL}{T}\right)^{-1}$$

Appendix B

Empirical Adjustment to Power Polar to Reflect Nonlinear Aerodynamics Region

Since these procedures are flap deflection angle dependent, this example is for the case of zero flap deflection (i.e., $\delta_f = 0$)

From Table 1, the average study values of C_p and C_w are -

$$\bar{C}_p = .001141 ; \bar{C}_w = .00977$$

From Figure 5, at $C_p = .001141$

$$\Delta C_w = .0003$$

Therefore, the linear C_w would equal the non-linear C_w study value plus the C_p dependent ΔC_w -

$$C_{w_{LIN}} = C_{w_{NONLIN}} + \Delta C_w \Big|_{C_p = .001141} \\ = .00977 + .0003$$

$$C_{w_{LIN}} = .01007$$

Next, the linear interpolation equation (Eqn. 8) is used to calculate the linear C_w value at a C_p of .001 -

$$C_{w_{LIN}} \Big|_{C_p = .001} = \left(\frac{.001 - .00012}{.001141 - .00012} \right)^{2/3} (.01007)$$

$$C_{w_{LIN}} = .00912$$

Finally, this linear C_w value, at the desired C_p , is then projected back to reflect the nonlinear relationship. From Figure 5, at $C_p = .001$ -

$$\Delta C_w = .00015$$

Then the final nonlinear C_w equals the linear interpolated C_w value minus the C_p dependent ΔC_w

$$C_{w_{\text{NONLIN}}} = C_{w_{\text{LIN}}} - \Delta C_w \Big|_{C_p=0.001}$$

$$= .00912 - .00015$$

$$C_{w_{\text{NONLIN}}} = .00897$$

Appendix C

**Development of the Biot-Savart Equation
to Determine the Axial Velocity
Component Due to a Vortex Ring**

Beginning with equation 15 -

$$\begin{aligned}
 \tilde{\rho}_x(x, r) &= \frac{-\Gamma}{4\pi r} \int_0^{2\pi} \frac{r \cos(\phi - \phi') - 1}{\sqrt{x^2 + r^2 + 1 - 2r \cos(\phi - \phi')}}^3 d\phi' \\
 &= \frac{-\Gamma}{4\pi r} \int_0^{2\pi} \frac{r \cos(\phi - \phi') - 1}{\sqrt{x^2 + r^2 + 1 - 2r \cos(\phi - \phi')}} \left[x^2 + r^2 + 1 - 2r \cos(\phi - \phi') \right]^3 d\phi' \\
 &= \frac{-\Gamma}{4\pi r} \int_0^{2\pi} \frac{(r \cos(\phi - \phi') - 1) d\phi'}{\sqrt{x^2 + r^2 + 2r + 1 - 2r[\cos(\phi - \phi') + 1]} \left[x^2 + r^2 - 2r + 1 + 2r[1 - \cos(\phi - \phi')] \right]} \\
 &= \frac{-\Gamma}{4\pi r} \int_0^{2\pi} \frac{(r \cos(\phi - \phi') - 1) d\phi'}{\sqrt{x^2 + (r+1)^2 - 2r[\cos(\phi - \phi') + 1]} \left[x^2 + (r-1)^2 + 2r[1 - \cos(\phi - \phi')] \right]} \\
 &= \frac{-\Gamma}{4\pi r} \frac{1}{\sqrt{x^2 + (r+1)^2 [x^2 + (r-1)^2]}} \int_0^{2\pi} \frac{(r \cos(\phi - \phi') - 1) d\phi'}{\sqrt{1 - \frac{2r[\cos(\phi - \phi') + 1]}{x^2 + (r+1)^2}} \left[1 + \frac{2r[1 - \cos(\phi - \phi')]}{x^2 + (r-1)^2} \right]}
 \end{aligned}$$

$$\text{Letting } I_1 = \int_0^{2\pi} \frac{(r \cos(\phi - \phi') - 1) d\phi'}{\sqrt{1 - \frac{2r[\cos(\phi - \phi') + 1]}{x^2 + (r+1)^2}} \left[1 + \frac{2r[1 - \cos(\phi - \phi')]}{x^2 + (r-1)^2} \right]}$$

then

$$\tilde{\rho}_x(x, r) = \frac{-\Gamma}{4\pi r} \frac{1}{\sqrt{x^2 + (r+1)^2 [x^2 + (r-1)^2]}} I_1$$

Now the expression for I_1 is developed -

$$I_1 = \int_0^{2\pi} \frac{r \cos(\phi - \phi') d\phi'}{\sqrt{1 - \frac{2r[\cos(\phi - \phi') + 1]}{x^2 + (r+1)^2}} \left[1 + \frac{2r[1 - \cos(\phi - \phi')]}{x^2 + (r-1)^2} \right]} - \int_0^{2\pi} \frac{d\phi'}{\sqrt{1 - \frac{2r[\cos(\phi - \phi') + 1]}{x^2 + (r+1)^2}} \left[1 + \frac{2r[1 - \cos(\phi - \phi')]}{x^2 + (r-1)^2} \right]}$$

For simplicity, the numerators and denominators will be developed separately. Beginning with the denominator,

$$\begin{aligned} & \frac{1}{\sqrt{1 - \frac{2r[\cos(\phi - \phi') + 1]}{x^2 + (r+1)^2}} \left[1 + \frac{2r[1 - \cos(\phi - \phi')]}{x^2 + (r-1)^2} \right]} \\ &= \frac{1}{\sqrt{1 - \frac{2r[\cos(\phi - \phi') + 1]}{x^2 + (r+1)^2}} \left[\frac{x^2 + (r-1)^2 + 2r[1 - \cos(\phi - \phi')]}{x^2 + (r-1)^2} \right]} \\ &= \frac{1}{\sqrt{1 - \frac{2r[\cos(\phi - \phi') + 1]}{x^2 + (r+1)^2}} \left[\frac{x^2 + r^2 - 2r + 1 - 2r + 2r + 2r[1 - \cos(\phi - \phi')]}{x^2 + r^2 - 2r + 1 - 2r + 2r} \right]} \\ &= \frac{1}{\sqrt{1 - \frac{2r[\cos(\phi - \phi') + 1]}{x^2 + (r+1)^2}} \left[\frac{x^2 + (r+1)^2 - 2r[\cos(\phi - \phi') + 1]}{x^2 + (r+1)^2 - 4r} \right]} \\ &= \frac{x^2 + (r+1)^2 - 4r}{\sqrt{1 - \frac{2r[\cos(\phi - \phi') + 1]}{x^2 + (r+1)^2}} \left[x^2 + (r+1)^2 - 2r[\cos(\phi - \phi') + 1] \right]} \end{aligned}$$

$$\begin{aligned}
 &= \frac{\frac{x^2 + (r+1)^2 - 4r}{x^2 + (r+1)^2}}{\sqrt{1 - \frac{2r[\cos(\phi - \phi') + 1]}{x^2 + (r+1)^2}} \left[\frac{x^2 + (r+1)^2 - 2r[\cos(\phi - \phi') + 1]}{x^2 + (r+1)^2} \right]} \\
 &= \frac{1 - \frac{4r}{x^2 + (r+1)^2}}{1 - \frac{2r[\cos(\phi - \phi') + 1]}{x^2 + (r+1)^2} \left[1 - \frac{2r[\cos(\phi - \phi') + 1]}{x^2 + (r+1)^2} \right]} \\
 &= \frac{1 - \frac{4r}{x^2 + (r+1)^2}}{\left[\sqrt{1 - \frac{4r[\frac{1 + \cos(\phi - \phi')}{2}]}{x^2 + (r+1)^2}} \right]^3} \\
 &= \frac{1 - \frac{4r}{x^2 + (r+1)^2}}{\left[\sqrt{1 - \frac{4r\cos^2(\frac{\phi - \phi'}{2})}{x^2 + (r+1)^2}} \right]^3}
 \end{aligned}$$

Letting $k^2 = \frac{4r}{x^2 + (r+1)^2}$

The integral has been reduced to -

$$I_1 = (1-k^2) \left[\int_0^{2\pi} \frac{r\cos(\phi - \phi') d\phi'}{\left[\sqrt{1 - k^2\cos^2(\frac{\phi - \phi'}{2})} \right]^3} - \int_0^{2\pi} \frac{d\phi'}{\left[\sqrt{1 - k^2\cos^2(\frac{\phi - \phi'}{2})} \right]^3} \right]$$

Now the numerator of the left hand integral is developed

$$\begin{aligned} r \cos(\phi - \phi') &= r(1 + \cos(\phi - \phi') - 1) \\ &= r \left[2 \left(\frac{1 + \cos(\phi - \phi')}{2} \right) - 1 \right] \end{aligned}$$

$$r \cos(\phi - \phi') = r \left[2 \cos^2 \left(\frac{\phi - \phi'}{2} \right) - 1 \right]$$

So the integral becomes -

$$I_1 = (1 - k^2) \left[\int_0^{2\pi} \frac{r [2 \cos^2 \left(\frac{\phi - \phi'}{2} \right) - 1]}{\sqrt{1 - k^2 \cos^2 \left(\frac{\phi - \phi'}{2} \right)}} d\phi' - \int_0^{2\pi} \frac{d\phi'}{\sqrt{1 - k^2 \cos^2 \left(\frac{\phi - \phi'}{2} \right)}} \right]$$

Now consider a change of variables -

$$\text{Let } \left(\frac{\phi - \phi'}{2} \right) = \left(\frac{\pi}{2} - \alpha \right)$$

$$\text{then } \cos \left(\frac{\phi - \phi'}{2} \right) = \cos \left(\frac{\pi}{2} - \alpha \right)$$

$$= \cos \cancel{\frac{\pi}{2}} \cos \alpha + \sin \cancel{\frac{\pi}{2}} \sin \alpha$$

$$\cos \left(\frac{\phi - \phi'}{2} \right) = \sin \alpha$$

$$\text{And } \cos^2 \left(\frac{\phi - \phi'}{2} \right) = \sin^2 \alpha$$

$$\text{Also for } \left(\frac{\phi - \phi'}{2} \right) = \left(\frac{\pi}{2} - \alpha \right) \Rightarrow \phi' = \phi - \pi + 2\alpha$$

$$d\phi' = 2 d\alpha$$

The change of variables affects the limits of integration as follows -

$$\text{For } \phi' = 0 \rightarrow \frac{\phi}{2} = \frac{\pi}{2} - \alpha \Rightarrow \alpha = \frac{\pi}{2} - \frac{\phi}{2}$$

$$\text{For } \phi' = 2\pi \Rightarrow \frac{\phi - 2\pi}{2} = \frac{\pi}{2} - \alpha \Rightarrow \alpha = \frac{3\pi}{2} - \frac{\phi}{2}$$

The path of integration from $(\frac{\pi}{2} - \frac{\phi}{2})$ to $(\frac{3\pi}{2} - \frac{\phi}{2})$ can be changed to from $(\frac{\pi}{2})$ to $(\frac{3\pi}{2})$ with no change

to the resultant value of the integral due to the periodic nature of the integrand and the fact that both paths cover π radians. By the same reasoning the path can also be changed to twice the value of the integral integrated from 0 to $\frac{\pi}{2}$ radians.

Making the above substitutions yields -

$$I_1 = (1-k^2) \left[2r(2) \int_0^{\pi/2} \frac{\sin^2 \alpha (2d\alpha)}{\sqrt{1-k^2 \sin^2 \alpha}} - r(2) \int_0^{\pi/2} \frac{2d\alpha}{\sqrt{1-k^2 \sin^2 \alpha}} \right. \\ \left. - (2) \int_0^{\pi/2} \frac{2d\alpha}{\sqrt{1-k^2 \sin^2 \alpha}} \right]$$

$$I_2 = (1-k^2) \left[2r(4) \int_0^{\pi/2} \frac{\sin^2 \alpha d\alpha}{\sqrt{1-k^2 \sin^2 \alpha}} - 4(r+1) \int_0^{\pi/2} \frac{d\alpha}{\sqrt{1-k^2 \sin^2 \alpha}} \right]$$

The resulting integrals are defined as complete elliptic integrals -

$$K(k) = \int_0^{\pi/2} \frac{d\alpha}{\sqrt{1-k^2 \sin^2 \alpha}} \quad (1st \text{ Kind})$$

$$E(k) = \int_0^{\pi/2} \sqrt{1-k^2 \sin^2 \alpha} d\alpha \quad (2nd \text{ Kind})$$

$$D(k) = \int_0^{\pi/2} \frac{\sin^2 \alpha d\alpha}{\sqrt{1-k^2 \sin^2 \alpha}} = \frac{K(k) - E(k)}{k^2}$$

Then using the relations (Ref. 2) -

$$\int_0^{\pi/2} \frac{d\alpha}{\left[\sqrt{1-k^2 \sin^2 \alpha} \right]^3} = \frac{E(k)}{1-k^2}$$

$$\int_0^{\pi/2} \frac{\sin^2 \alpha d\alpha}{\left[\sqrt{1-k^2 \sin^2 \alpha} \right]^3} = \frac{K(k) - D(k)}{1-k^2}$$

The expression for I_1 then becomes -

$$I_1 = (1-k^2) \left[2r(4) \left(\frac{K(k) - D(k)}{1-k^2} \right) - (4)(r+1) \sqrt{\frac{E(k)}{1-k^2}} \right]$$

$$I_1 = 2r(4)(K(k) - D(k)) - 4(r+1)(E(k))$$

And the relation for the axial velocity becomes -

$$v_{\delta x}(x, r) = - \frac{\Gamma}{2\pi r'} \frac{4r(K(k) - D(k)) - 2(r+1)(E(k))}{\sqrt{x^2 + (r+1)^2} [x^2 + (r-1)^2]}$$

This expression is now developed further -

$$v_{\delta x}(x, r) = - \frac{\Gamma}{2\pi r' \sqrt{x^2 + (r+1)^2}} \left\{ \frac{4r(K(k) - D(k))}{x^2 + (r-1)^2} - \frac{2(r+1)E(k)}{x^2 + (r-1)^2} \right\}$$

$$= \frac{\Gamma}{2\pi r' \sqrt{x^2 + (r+1)^2}} \left\{ \frac{2(r+1)E(k)}{x^2 + (r-1)^2} - \frac{4r(K(k) - D(k))}{x^2 + (r-1)^2} \right\}$$

$$\text{Letting } A = \frac{\Gamma}{2\pi r' \sqrt{x^2 + (r+1)^2}}$$

Then -

$$v_{\delta x}(x, r) = A \left\{ \frac{2(r+1)E(k)}{x^2 + (r-1)^2} - \frac{4r(K(k) - \frac{K(k) - E(k)}{k^2})}{x^2 + (r-1)^2} \right\}$$

$$\begin{aligned}
 &= A \left\{ \frac{2(r+1)E(k)}{x^2 + (r-1)^2} - \frac{4r(k^2 K(k) - K(k) + E(k))}{k^2(x^2 + (r-1)^2)} \right\} \\
 &= A \left\{ \frac{2(r+1)E(k)}{x^2 + (r-1)^2} - \frac{4r[(k^2 - 1)K(k) + E(k)]}{k^2(x^2 + (r-1)^2)} \right\}
 \end{aligned}$$

Realizing that $k^2 - 1 = -\frac{x^2 + (r-1)^2}{x^2 + (r+1)^2}$

And substituting this in gives -

$$\begin{aligned}
 N_{\delta x}(x, r) &= A \left\{ \frac{2(r+1)E(k)}{x^2 + (r-1)^2} - \frac{4r \left[\left(-\frac{x^2 + (r-1)^2}{x^2 + (r+1)^2} \right) K(k) + E(k) \right]}{k^2(x^2 + (r-1)^2)} \right\} \\
 &= A \left\{ \frac{2(r+1)E(k)}{x^2 + (r-1)^2} - \frac{4r \left(-\frac{x^2 + (r-1)^2}{x^2 + (r+1)^2} K(k) \right)}{k^2(x^2 + (r-1)^2)} - \frac{4r E(k)}{k^2(x^2 + (r-1)^2)} \right\}
 \end{aligned}$$

Realizing that $k^2 = \frac{4r}{x^2 + (r+1)^2}$

Substituting this in and cancelling terms gives -

$$\begin{aligned}
 N_{\delta x}(x, r) &= A \left\{ \frac{2(r+1)E(k)}{x^2 + (r-1)^2} + K(k) - \frac{x^2 + (r+1)^2}{x^2 + (r-1)^2} E(k) \right\} \\
 &= A \left\{ K(k) + \left[\frac{2r+2-x^2-r^2-2r-1}{x^2+(r-1)^2} \right] E(k) \right\} \\
 &= A \left\{ K(k) + \left[\frac{(-x^2-r^2+2r-1)-2r+2}{x^2+(r-1)^2} \right] E(k) \right\} \\
 &= A \left\{ K(k) + \left[\frac{(-x^2-(r-1)^2)-2(r+1)}{x^2+(r-1)^2} \right] E(k) \right\}
 \end{aligned}$$

$$\begin{aligned}
 &= A \left\{ K(k) + \left[-\frac{x^2 + (r-1)^2}{x^2 + (r-1)^2} - \frac{2(r+1)}{x^2 + (r-1)^2} \right] E(k) \right\} \\
 &= A \left\{ K(k) + \left[-1 - \frac{2(r+1)}{x^2 + (r-1)^2} \right] E(k) \right\} \\
 &= A \left\{ K(k) - \left[1 + \frac{2(r+1)}{x^2 + (r-1)^2} \right] E(k) \right\}
 \end{aligned}$$

So the final form of the axial velocity equation to be solved takes the form -

$$\omega_{dx}(x, r) = \frac{\Gamma}{2\pi r \cdot x^2 + (r+1)^2} \left\{ K(k) - \left[1 + \frac{2(r+1)}{x^2 + (r-1)^2} \right] E(k) \right\}$$

Appendix D
Calibration Version of XV-15
Computer Program

ORIGINAL PAGE IS
OF POOR QUALITY

```

=====
C THIS PROGRAM IS DESIGNED TO SIMULATE THE XV-15 ROTOR SYSTEM PERFORMANCE
C THROUGH THE USE OF A VORTEX RING ANALYSIS. THIS PROGRAM IS BASED ON
C A CONSTANT ROTOR TIP SPEED OF 768.38 FT/SEC AND CAN PERFORM THE
C ANALYSIS FOR THREE DIFFERENT THRUST COEFFICIENTS (.0094,.01,.0105).
C THIS PARTICULAR PROGRAM VERSION WAS DESIGNED TO CALIBRATE THE VORTEX
C RING SPACING FACTOR (K) AND HENCE MODELS ONLY ONE ROTOR OF THE SIDE
C BY SIDE ROTOR SYSTEM. THE VALUE FOR K IS AN INPUT PARAMETER IN THIS
C PROGRAM AND IS VARIED UNTIL AN AVERAGE INFLOW VELOCITY THAT AGREES
C WITH THAT PREDICTED BY SIMPLE MOMENTUM THEORY. I.e.,  $V = V_{tip} C_t / 2.005$ .
C IS OBTAINED.
C DUE TO THE FACT THAT THE AVERAGE INFLOW VELOCITY AT THE ROTOR DISK
C IS WHAT'S DESIRED, THE POINTS AT WHICH THE VELOCITIES ARE CALCULATED
C LIE ALONG A LINE WHICH IS COINCIDENTAL WITH THE ROTOR PLANE.
C
C=====
C
C
C LIST OF VARIABLES:
C
C K.....VORTEX RING SPACING FACTOR
C B.....ROTOR SPEED (SEC/REV)
C F(1)....TIME BETWEEN VORTEX RINGS (SEC)
C (BASED ON THREE RINGS PER REVOLUTION)
C KT(1)....CORRECTED TIME BETWEEN VORTEX RINGS (SEC)
C (K=F(1))
C Z(1)....THE POSITION OF EACH VORTEX RING, DOWNSTREAM
C OF THE ROTOR DISK, AS A FUNCTION OF CORRECTED
C TIME (FT)
C RR(1)....VORTEX RING RADIUS (FT)
C (A FUNCTION OF ROTOR GEOMETRY AND DOWNSTREAM
C POSITION)
C TWR.....THE TOTAL NUMBER OF VORTEX RINGS CONSIDERED
C IN THE ANALYSIS
C A.....THE VORTEX RING CIRCULATION (FT**2/SEC)
C CT.....THRUST COEFFICIENT (THRUST/(RHO*AREA*Vtip**2.))
C L.....THE DISTANCE BETWEEN THE ROTOR AXIS AND THE
C POINT WHERE THE AXIAL VELOCITIES ARE BEING
C CALCULATED (FT)
C J.....THE ABSOLUTE VALUE OF POINT (FT)
C X.....THE RATIO OF VORTEX RING DOWNSTREAM POSITION
C TO RING RADIUS (Z(1)/RR(1))
C R.....THE RATIO OF J TO THE RING RADIUS
C (RAD/RR(1))
C S.T.U.E.B.C.CIRC..COMPONENTS OF THE EQUATION USED TO DETERMINE
C THE AXIAL VELOCITY DUE TO EACH RING (FROM:
C "AERODYNAMICS OF PROPULSION", KUCHEMANN & WEBER,
C 1953)
C P.D.....INTERMEDIATE STORAGE VARIABLES
C V(M,N)....THE COMPONENT OF THE AXIAL VELOCITY AT POINT
C M DUE TO RING N (FT/SEC)
C VTOT(1)....THE TOTAL AXIAL VELOCITY AT EACH OF 31 POINTS
C DUE TO SUMMING THE COMPONENTS FROM EACH VORTEX
C RING (FT/SEC)

```

ORIGINAL PAGE IS
OF POOR QUALITY

```
C      VAVC.....THE SUM OF THE AXIAL VELOCITIES ALONG THE ROTOR
C      DISK (FT/SEC)
C      VDISK.....THE AVERAGE INFLOW VELOCITY ALONG THE ROTOR DISK
C      (FT/SEC)
C
C*****
C
C      INTEGER TNR
C      REAL    K,KT(72),RR(72),Z(72),F(72),VTOT(31),V(31,72)
C
C*****
C
C      THE VALUE TO BE USED FOR THE VORTEX RING SPACING FACTOR (K) IS
C      FIRST READ IN AND THE USER IS PROMPTED FOR THE DESIRED THRUST
C      COEFFICIENT (CT).
C
C*****
C
C      WRITE(6,4)
4     FORMAT(' WHAT K VALUE WILL BE USED?')
READ(5,5)K
5     FORMAT(C12.5)
WRITE(6,9)
9     FORMAT(' WHAT THRUST COEFFICIENT (CT) WILL BE USED?')
WRITE(6,11)
11    FORMAT(' (.0094,.01,.0105)?')
READ(5,10)CT
10    FORMAT(C12.5)
C
C*****
C
C      NEXT, BASED ON A ROTOR SPEED OF 760.38 FT/SEC (.1022 SEC/REV), THE
C      TIME SPACING OF THE VORTEX RINGS IS CALCULATED USING THE INPUT RING
C      SPACING FACTOR (K).
C
C*****
C
C      B=.1022
DO 20 I=1,72
      F(I)=I*B/3.0
      KT(I)=K*F(I)
20    CONTINUE
C
C*****
C
C      DEPENDING ON WHICH THRUST COEFFICIENT WAS SELECTED, AN IF/THEN
C      STATEMENT SETS THE PROPER VALUE OF VORTEX RING CIRCULATION AND
C      TRANSFERS CONTROL TO THE APPROPRIATE INTERPOLATING POLYNOMIAL.
C
```

ORIGINAL PAGE IS
OF POOR QUALITY

```

C
C-----*
C
C      IF(CT.EQ..0094) THEN
C          A=189.08
C          GO TO 23
C      ENDIF
C      IF(CT.EQ..01) THEN
C          A=201.16
C          GO TO 30
C      ENDIF
C      IF(CT.EQ..0105) THEN
C          A=211.22
C          GO TO 35
C      ENDIF
C
C-----*
C
C      DEPENDING ON WHICH THRUST COEFFICIENT WAS SELECTED, ONE OF THREE
C      INTERPOLATING POLYNOMIALS IS USED TO CALCULATE THE DOWNSTREAM
C      POSITION OF EACH VORTEX RING AS A FUNCTION OF TIME. EACH VORTEX
C      RING'S RADIUS IS ALSO CALCULATED AS A FUNCTION OF RING DOWNSTREAM
C      POSITION.
C
C-----*
C
C      DO 40 I=1,72
C          Z(I)=-69.855*KT(I)**5.+208.424*KT(I)**4.-242.599*KT(I)**3.
C          + 120.798*KT(I)**2.+75.912*KT(I)
C          RR(I)=8.8375*SQRT(1./(.5*(2.-EXP(-.09512*Z(I)))))
C 40      CONTINUE
C          GO TO 24
C
C-----*
C
C      DO 45 I=1,72
C          Z(I)=-68.152*KT(I)**5.+221.77*KT(I)**4.-236.836*KT(I)**3.
C          + 126.62*KT(I)**2.+78.082*KT(I)
C          RR(I)=8.8375*SQRT(1./(.5*(2.-EXP(-.09512*Z(I)))))
C 45      CONTINUE
C          GO TO 24
C
C-----*
C
C      DO 50 I=1,72
C          Z(I)=-64.746*KT(I)**5.+211.756*KT(I)**4.-247.219*KT(I)**3.
C          + 123.687*KT(I)**2.+81.398*KT(I)
C          RR(I)=8.8375*SQRT(1./(.5*(2.-EXP(-.09512*Z(I))))
C 50      CONTINUE
C
C-----*
C
C      THE TOTAL NUMBER OF RINGS TO BE USED FOR THE ANALYSIS (TMR) AND
C      THE POSITION OF THE FIRST POINT, AT WHICH THE AXIAL VELOCITIES ARE

```

ORIGINAL PAGE IS
OF POOR QUALITY

```

C      TO BE CALCULATED, WITH RESPECT TO THE ROTOR AXIS ARE READ IN.
C
C*****
C
24      TNR=72
        L=-15
C
C*****
C
C      TWO DO LOOPS ARE USED TO CALCULATE EACH VORTEX RING'S AXIAL.
C      VELOCITY COMPONENT AT EACH POINT OF INTEREST. THE INNER LOOP
C      CALCULATES THE VELOCITIES FROM EACH OF THE RINGS AND THE OUTER LOOP
C      INCREMENTS THE POINT AT WHICH THE VELOCITIES ARE CALCULATED.
C
C*****
C
C      DO 65 M=1,31
C
C      DO 70 N=1,TNR
        IF(L.LT.0)J=-L
        IF(L.GE.0)J=L
        X=-Z(N)/RR(N)
        R=J/RR(N)
        S=(4.*R)/(X**2.+(R+1.)**2.)
        T=ALOC(4./(1.-S)**.5)
        U=T*((T-1.)/4.)*(1.-S)+(9./64.)*(T-(7./6.))*(1.-S)**2.
        E=1.+(.5*(T-.5)*(1.-S))+(3./16.)*(T-(13./12.))*(1.-S)**2.
        B=1./(X**2.+(R+1.)**2.)**.5
        C=(1.+((2.*R-1.)/(X**2.+(R-1.)**2.)))
        D=U+C*E
        P=B*D
        CIRC=A/(2.*3.14159*RR(N))
        V(M,N)=CIRC*P
70      CONTINUE
C
        L=L+1
C
65      CONTINUE
C
C*****
C
C      THE VELOCITY COMPONENTS DUE TO EACH OF THE VORTEX RINGS ARE NOW
C      SUMMED TO ARRIVE AT A TOTAL AXIAL VELOCITY AT EACH POINT OF
C      INTEREST
C
C*****
C
C      DO 75 J=1,31
        DO 76 I=1,TNR
          VTOT(J)=VTOT(J)+V(J,I)
76      CONTINUE

```

ORIGINAL PAGE IS
OF POOR QUALITY

```
73    CONTINUE
C
C*****C
C
C      THE TOTAL AXIAL VELOCITY AT EACH POINT OF INTEREST IS NOW PRINTED
C      OUT ALONG WITH THE ASSOCIATED VALUE OF VORTEX RING SPACING FACTOR
C      (K), THRUST COEFFICIENT (CT), AND THE NUMBER OF VORTEX RINGS USED.
C
C*****C
C
C      WRITE(6,85)K,CT,TNR
85    FORMAT(1X,' FOR K=' ,F7.6,' , CT=' ,F5.4,
+' AND' ,1X,12,' VORTEX RINGS')
      WRITE(6,90)
90    FORMAT(1X,' THE TOTAL AXIAL VELOCITY AT EACH POINT ALONG A LINE')
      WRITE(6,93)
93    FORMAT(1X,' COINCIDENTAL WITH THE PLANE OF THE ROTOR IS:')
      DO 97 J=1,31
        WRITE(6,96)J,VTOT(J)
96    FORMAT(1X,2X,3BVTOT(.12,2H)=,C12.5)
97    CONTINUE
C
C*****C
C
C      SINCE FOR CALIBRATION PURPOSES THE AVERAGE VELOCITY ALONG THE ROTOR
C      DISK IS WHAT'S OF PRIME IMPORTANCE, THAT VALUE IS NOW CALCULATED
C      AND OUTPUT.
C
C*****C
C
C      DO 69 I=4,28
69    VAVC=VAVC+VTOT(I)
      CONTINUE
      VDISK=VAVC/25.0
      WRITE(6,71)VDISK
71    FORMAT(1X,' THE AVERAGE INFLOW VELOCITY IS' ,1X,F5.2,' FT/SEC')
      STOP
      END
```

Appendix E
Download Version of XV-15
Computer Program

ORIGINAL PAGE IS
OF POOR QUALITY

```

C
C
C THIS PROGRAM IS DESIGNED TO SIMULATE THE PROPULSION SYSTEM OF THE
C XV-15 AIRCRAFT, THROUGH THE USE OF A VORTEX RING ANALYSIS. FOR THE
C PURPOSE OF DETERMINING THE ROTOR GENERATED WING DOWNLOAD THAT OCCURS
C IN THE HOVER CONFIGURATION. THE PROGRAM IS BASED ON A CONSTANT ROTOR
C TIP SPEED OF 768.38 FT/SEC AND UTILIZES THE PREDETERMINED VORTEX RING
C SPACING FACTOR K. THE PROGRAM COMPUTES THE AXIAL VELOCITY COMPONENTS
C DUE TO EACH VORTEX RING AT A POSITION WHERE THE AIRCRAFT WING WOULD
C BE, 4.67 DOWNSTREAM FROM THE ROTOR DISKS. THE COMPUTATION IS BEGUN
C 35 FEET FROM THE AIRCRAFT LONGITUDINAL CENTERLINE AND PROCEEDS IN
C 1 FOOT INCREMENTS UNTIL A POSITION 35 FEET ON THE OPPOSITE SIDE OF
C THE AIRCRAFT CENTERLINE IS REACHED. THE AXIAL VELOCITY COMPONENTS
C FROM EACH VORTEX RING BEING CALCULATED AT EACH OF THE INCREMENTAL
C STEPS. THE TOTAL VELOCITY, THE SUMMATION OF ALL THE AXIAL COMPONENTS
C IS THEN AVERAGED BETWEEN EACH TWO SUCCESSIVE POINTS AND THIS AVERAGED
C VELOCITY IS THEN USED TO CALCULATE A FORCE (DOWNLOAD) COMPONENT.
C THE FORMULA USED IS:  $F = 5 * RHO * VBAR^2 * S * C4$ . THE SURFACE
C AREA (S) IN THE FORMULA IS TAKEN TO BE A 1 FOOT CHORD SECTION
C MULTIPLIED BY THE AIRCRAFT WING CHORD, 5.23 FEET. THE DOWNLOAD
C COMPUTATION IS ONLY PERFORMED USING THE COMPUTED VELOCITIES THAT
C LIE BETWEEN THE ROTOR CENTERLINES. THIS BEING THE ONLY AREA THAT IS
C ACTUALLY AIRCRAFT WING. THE DOWNLOAD IS THEN SUMMED AND DIVIDED BY
C THE TOTAL ROTOR PRODUCED THRUST TO ARRIVE AT DOWNLOAD AS A PERCENT OF
C ROTOR THRUST. THE PROGRAM IS DESIGNED TO SIMULATE A NUMBER OF HOVER
C CONFIGURATIONS. ANY OF THREE THRUST COEFFICIENTS (.0094, .01, .0185)
C CAN BE USED AS ANY OF FOUR ROTOR HEIGHT ABOVE GROUND TO ROTOR DIAMETER
C (H/D) RATIOS (H/D=INFINITY (OUT OF GROUND EFFECT, OGE), H/D=2.0 (IN GROUND
C EFFECT, ICE), H/D=1.0 (ICE), AND H/D=0.9 (ICE)). THE PROGRAM ALSO MAKES
C USE OF DRAG COEFFICIENTS DETERMINED FROM WIND TUNNEL TESTS IN WHICH
C A WING, REPRESENTATIVE OF THE XV-15 WING, WAS ALIGNED WITH ITS CHORD
C PERPENDICULAR TO THE FREE STREAM VELOCITY. THE WING WAS EQUIPPED
C WITH FLAPS. ALSO REPRESENTATIVE OF THE XV-15, AND TESTED SO AS TO
C DETERMINE DRAG COEFFICIENTS CORRESPONDING TO DIFFERENT DEGREES OF FLAP
C DEFLECTION. THE DRAG COEFFICIENTS ARE UTILIZED HERE AND HENCE GIVE
C THE PROGRAM THE CAPABILITY OF ANALYZING ANY OF FIVE FLAP DEFLECTION
C CONFIGURATIONS (0, 20, 40, 60 & 80 DEGREES).
C
C ****
C
C
C ****
C
C
C LIST OF VARIABLES:
C
C CT.....THRUST COEFFICIENT ( $T/(RHO*A*V^2)$ )
C H/D.....ROTOR RECENT ABOVE GROUND PLANE TO ROTOR
C          DIAMETER RATIO
C FLAPSET.....THE DEGREES OF WING FLAP DEFLECTION (DEC)
C CD.....DRAG COEFFICIENT
C A.....VORTEX RING CIRCULATION (FT2/SEC)
C K.....VORTEX RING SPACING FACTOR
C H.....ROTOR SPEED (SEC/REV)
C F(1).....TIME BETWEEN ROTOR BLADE PASSAGES (SEC/REV)
C KT(1).....CORRECTED TIME BETWEEN VORTEX RING SHEDDING
C          ( $K * F(1)$ ) (SEC/REV)
C Z(1).....THE POSITION OF EACH VORTEX RING, DOWNSTREAM OF

```

C - 2

```

C THE ROTOR DISK, AS A FUNCTION OF CORRECTED TIME
C (FT)
C RR(1).....VORTEX RING RADIUS (FT) (A FUNCTION OF ROTOR
C GEOMETRY AND VORTEX RING DOWNSTREAM POSITION
C COORD(I).....THE DOWNSTREAM POSITION OF THE VORTEX RINGS WITH
C RESPECT TO THE XV-15 WING POSITION (FT)
C HOVERD.....THE RATIO OF ROTOR HEIGHT ABOVE GROUND PLANE
C TO ROTOR DIAMETER (H/D)
C NUMRINC.....THE NUMBER OF VORTEX RINGS, FOR AN IN GROUND
C EFFECT (ICE) HOVER CONDITION, THAT ARE NEEDED TO
C SATISFY THE PRESCRIBED ROTOR HEIGHT TO DIAMETER
C RATIO POSITIONING OF THE GROUND PLANE.
C TMR.....THE TOTAL NUMBER OF VORTEX RINGS USED IN THE
C ANALYSIS (DICTATED BY THE HOVER CONDITION)
C TWICENR.....THE NUMBER OF THE VORTEX RING THAT CORRESPONDS
C TO THE MIRROR IMAGE OF THE FIRST VORTEX RING
C FROM THE RIGHT ROTOR (ICE HOVER)
C THREEENR.....THE NUMBER OF THE FIRST VORTEX RING FROM THE LEFT
C ROTOR (ICE HOVER)
C RS.....THE TOTAL NUMBER OF VORTEX RINGS ON THE RIGHT SIDE
C (ICE HOVER)
C LS.....THE NUMBER OF THE FIRST VORTEX RING ON THE LEFT SIDE
C (ICE HOVER)
C L.....THE DISTANCE FROM THE AIRCRAFT LONGITUDINAL CENTER-
C LINE TO THE POINT AT WHICH THE AXIAL VELOCITIES ARE
C CALCULATED (FT)
C RAD.....THE DISTANCE FROM THE AIRCRAFT LONGITUDINAL CENTER-
C LINE TO THE ROTOR CENTERLINES (FT)
C X.....THE RATIO OF VORTEX RING DOWNSTREAM POSITION TO RING
C RADIUS (Z(1)/RR(1))
C R.....THE RATIO OF THE DISTANCE, FROM THE POINT AT WHICH
C THE VELOCITIES ARE TO BE CALCULATED TO THE ROTOR
C CENTERLINES, TO THE RING'S RADI
C S.T.U.E.B.C.CIRC..COMPONENTS OF THE EQUATION USED TO DETERMINE THE
C AXIAL VELOCITY COMPONENTS DUE TO EACH RING (FROM
C "AERODYNAMICS OF PROPULSION", KUCHIEMANN & WEBER, 1953)
C P,D.....INTERMEDIATE STORAGE VARIABLES
C V(M,N).....THE COMPONENT OF THE AXIAL VELOCITY AT POINT M DUE TO
C RING N (FT/SEC)
C VTOT(J).....THE TOTAL AXIAL VELOCITY AT EACH OF 71 POINTS DUE TO
C SUMMING THE COMPONENTS FROM EACH VORTEX RING (FT/SEC)
C VBAR.....THE VELOCITY OBTAINED BY AVERAGING THE TOTAL AXIAL
C VELOCITIES AT TWO SUCCESSIVE POINTS (FT/SEC)
C DWNLD1.....THE FORCE (DOWNLOAD) OBTAINED BY USING VBAR AND A
C 5.25 SQ. FOOT WING SECTIONAL AREA (LD)
C (DWNLD1=.5*RD0*VBAR**2.*5.25*CD)
C DWNLD2.....THE SUM OF THE INDIVIDUAL DOWNLOAD COMPONENTS (LB)
C PRCHDLT.....THE PERCENTAGE OF TOTAL ROTOR THRUST THAT IS DOWN-
C LOAD ((DWNLD2/TURUST)*100.) (TURUST=f(CT))

C ****
C
C INTEGER TWICENR,THREEENR,TMR,Y,NUMRINC,RS,LS,FLAPSET
C REAL K,KT(72),ZAC,LAC
C DIMENSION Z(144),COORD(144),F(72),RR(144),VTOT(71),V(71,144)
C
C ****

```

```
C THE USER IS FIRST PROMPTED FOR THE DESIRED THRUST COEFFICIENT (CT),
C ROTOR HEIGHT ABOVE GROUND PLANE TO ROTOR DIAMETER RATIO (H/D), AND
C FLAP SETTING (FLAPSET)
C
C*****C
C
C      WRITE(6,9)
9     FORMAT(' WHAT THRUST COEFFICIENT (CT) WILL BE USED?')
WRITE(6,11)
11    FORMAT(' (.0094..01..0105)?')
READ(5,10)CT
10    FORMAT(C12.5)
WRITE(6,16)
16    FORMAT(' WHAT H/D RATIO WILL BE USED?')
WRITE(6,14)
14    FORMAT(' (0.5,1.0,2.0, OR OCE.HOVERD)')
WRITE(6,17)
17    FORMAT(' (ENTER 0.0 FOR OCE HOVER)')
READ(5,18)HOVERD
18    FORMAT(C12.5)
WRITE(6,19)
19    FORMAT(' WHAT FLAP SETTING WILL BE USED?')
WRITE(6,15)
15    FORMAT(' (0.20,40,45,60 DEC.)')
READ(5,8)FLAPSET
8     FORMAT(I2)
C
C*****C
C
C      FROM THE SELECTED FLAP SETTING, THE PROPER DRAG COEFFICIENT IS SET
C
C*****C
C
C      IF(FLAPSET.EQ.0) THEN
CD=1.70
ENDIF
IF(FLAPSET.EQ.20) THEN
CD=1.52
ENDIF
IF(FLAPSET.EQ.40) THEN
CD=1.32
ENDIF
IF(FLAPSET.EQ.45) THEN
CD=1.26
ENDIF
IF(FLAPSET.EQ.60) THEN
CD=1.08
ENDIF
C
C*****C
C
C      THE VALUES FOR VORTEX RING CIRCULATION (A) AND VORTEX RING SPACING
```

```

C   FACTOR (K) ARE NOW SET CORRESPONDING TO THE SELECTED THRUST COEFFICIENT
C
C*****
C
C   IF(CT.EQ..0094) THEN
A=189.08
K=.446
ENDIF
IF(CT.EQ..01) THEN
A=201.16
K=.446
ENDIF
IF(CT.EQ..0105) THEN
A=211.22
K=.442
ENDIF
C
C*****
C
C   SINCE THE AIRCRAFT HAS A THREE BLADED ROTOR, THREE VORTEX RINGS ARE
C   CONTINUOUSLY SHED FROM THE ROTOR IN A HELICAL SHAPE. AN APPROXIMATION
C   IS MADE HERE THAT TRANSFORMS THE THREE CONTINUOUS HELICAL VORTICES
C   INTO THREE ROUND VORTEX RINGS, EVENLY SPACED IN TIME AND SPACE. OVER
C   ONE ROTOR REVOLUTION, THE VORTEX RINGS' POSITION IN TIME IS THEN
C   ALTERED BY THE APPROPRIATE VORTEX RING SPACING FACTOR (K) THAT WAS
C   PREDETERMINED USING THE CALIBRATION PROGRAM VERSION
C
C*****
C
C   H=.1022
DO 20 I=1,72
      F(I)=I*B/3.0
      KT(I)=K*F(I)
20  CONTINUE
C
C*****
C
C   DEPENDING ON WHICH THRUST COEFFICIENT WAS SELECTED, CONTROL IS NOW
C   TRANSFERRED TO AN APPROPRIATE FIFTH ORDER INTERPOLATING POLYNOMIAL.
C   THE POLYNOMIALS ARE USED TO SET THE DOWNSTREAM POSITION OF EACH VORTEX
C   RING AS A FUNCTION OF THEIR RESPECTIVE CORRECTED TIME SPACING. THE
C   RADII OF EACH VORTEX RING IS ALSO CALCULATED, THESE BEING A FUNCTION
C   OF THE RING'S DOWNSTREAM POSITION AS WELL AS THE ROTOR'S DIAMETER.
C   THE POSITION OF EACH RING WITH RESPECT TO THE AIRCRAFT WING IS ALSO
DETERMINED.
IF ONE OF THE ICE HOVER CONDITIONS IS BEING ANALYZED, CONTROL IS
TRANSFERRED TO ANOTHER SECTION OF THE PROGRAM WHEN THE DOWNSTREAM
POSITION OF A VORTEX RING CLOSELY, IF NOT EXACTLY, SATISFIES THE
PREScribed H/D RATIO.
C
C*****
C

```

ORIGINAL PAGE IS
OF POOR QUALITY

```

C           IF(CT.EQ..01) GO TO 30
C           IF(CT.EQ..0105) GO TO 35
C
C 23   DO 40 I=1,36
      Z(I)=63.855*KT(I)**5.+208.424*KT(I)**4.-242.599*KT(I)**3.
      +126.798*KT(I)**2.+73.912*KT(I)
      RR(I)=8.8375*SORT(1./(.5*(2.-EXP(-.09512*Z(I)))))
      COORD(I)=Z(I)-4.67
      IF((HOVERD.EQ.0.5).AND.(Z(I).GE.12.5).OR.
      +(HOVERD.EQ.1.0).AND.(Z(I).GE.25.).OR.
      +(HOVERD.EQ.2.0).AND.(Z(I).GE.50.)) THEN
      NUMRINC=1
      ZAC=Z(I)
      GO TO 26
      ENDIF
  40   CONTINUE
      GO TO 24
C
C
C 30   DO 45 I=1,36
      Z(I)=68.152*KT(I)**5.+221.77*KT(I)**4.-236.836*KT(I)**3.
      +126.62*KT(I)**2.+78.083*KT(I)
      RR(I)=8.8375*SORT(1./(.5*(2.-EXP(-.09512*Z(I)))))
      COORD(I)=Z(I)-4.67
      IF((HOVERD.EQ.0.5).AND.(Z(I).GE.12.5).OR.
      +(HOVERD.EQ.1.0).AND.(Z(I).GE.25.).OR.
      +(HOVERD.EQ.2.0).AND.(Z(I).GE.50.)) THEN
      NUMRINC=1
      ZAC=Z(I)
      GO TO 26
      ENDIF
  45   CONTINUE
      GO TO 24
C
C
C 35   DO 50 I=1,36
      Z(I)=64.746*KT(I)**5.+211.756*KT(I)**4.-247.219*KT(I)**3.
      +123.687*KT(I)**2.+81.398*KT(I)
      RR(I)=8.8375*SORT(1./(.5*(2.-EXP(-.09512*Z(I))))
      COORD(I)=Z(I)-4.67
      IF((HOVERD.EQ.0.5).AND.(Z(I).GE.12.5).OR.
      +(HOVERD.EQ.1.0).AND.(Z(I).GE.25.).OR.
      +(HOVERD.EQ.2.0).AND.(Z(I).GE.50.)) THEN
      NUMRINC=1
      ZAC=Z(I)
      GO TO 26
      ENDIF
  50   CONTINUE
C
C
C ****
C
C
C     IF AN OCE HOVER CONDITION IS BEING ANALYZED, THIS SECTION PRODUCES
C     THE VORTEX RING SYSTEM FOR THE LEFT ROTOR.  THIS LEFT ROTOR VORTEX
C     RING SYSTEM IS IDENTICAL TO THE RIGHT EXCEPT FOR THE FACT THAT ITS
C     CENTERLINE COINCIDES WITH THAT OF THE LEFT ROTOR.  CONTROL IS TURE

```

ORIGINAL PAGE IS
OF POOR QUALITY

```
C      TRANSFERRED TO STATEMENT LABEL 60.  
C  
C*****  
C  
24    DO 41 I=1,36  
      Z(36+I)=Z(I)  
      RR(36+I)=RR(I)  
      COORD(36+I)=COORD(I)  
41    CONTINUE  
      TNR=72  
      GO TO 60  
C  
C*****  
C  
C      IF AN ICE ROVER CONDITION IS BEING ANALYZED, CONTROL IS TRANSFERRED  
C      TO THIS SECTION FROM THE INTERPOLATING POLYNOMIALS. THIS SECTION  
C      PRODUCES THE MIRROR IMAGE OF THE VORTEX RING SYSTEM ON THE RIGHT  
C      SIDE, REFLECTED ABOUT THE GROUND PLANE DICTATED BY THE B/D RATIO.  
C      ONCE THIS IS ACCOMPLISHED, AN IDENTICAL VORTEX RING SYSTEM IS PRO-  
C      DUCED FOR THE LEFT SIDE.  
C      THE FIRST SECTION SUPERIMPOSES A VORTEX RING, IDENTICAL IN RADIUS  
C      AND POSITION, ONTO THE LAST RING THAT WAS PRESCRIBED FROM THE INTER-  
C      POLATING POLYNOMIAL, i.e., THE RING THAT SATISFIES THE B/D RATIO.  
C  
C*****  
C  
26    Y=NUMRING+1  
      Z(Y)=Z(NUMRING)  
      RR(Y)=RR(NUMRING)  
      COORD(Y)=COORD(NUMRING)  
C  
C*****  
C  
C      THIS DO LOOP PRODUCES THE REMAINING 'MIRRORED' VORTEX RING SYSTEM-  
C      BEGINNING AFTER THE TWO SUPERIMPOSED VORTEX RINGS. THE FIRST RING  
C      PRODUCED BY THIS SECTION IS IDENTICAL IN RADIUS AND POSITION, WITH  
C      RESPECT TO THE SUPERIMPOSED RINGS, AS THE RING THAT OCCURS PRIOR  
C      TO THE SUPERIMPOSED RINGS. HENCE, THIS SECTION PRODUCES A SET OF  
C      VORTEX RINGS THAT ARE IDENTICAL IN RADIUS AND POSITION WITH RESPECT  
C      TO THE SUPERIMPOSED RINGS, i.e., GROUND PLANE.  
C  
C*****  
C  
C      DO 27 I=2,NUMRING  
      LOPE=I+NUMRING  
      LIP=Y-I  
      Z(LOPE)=Z(Y)+(Z(Y)-Z(LIP))  
      RR(LOPE)=RR(LIP)  
      COORD(LOPE)=Z(LOPE)-4.67  
27    CONTINUE  
C
```

ORIGINAL PAGE IS
OF POOR QUALITY

```
C*****
C
C
C      THIS SECTION PRODUCES A VORTEX RING SYSTEM FOR THE LEFT SIDE THAT
C      IS IDENTICAL TO THAT PREVIOUSLY PRODUCED FOR THE RIGHT SIDE.
C
C*****
C
C      TWICENR=2*NUMRING
C      THREEENR=3*NUMRING
C      TNR=4*NUMRING
C      DO 28 I=1,TWICENR
C          Z(I+TWICENR)=Z(I)
C          RR(I+TWICENR)=RR(I)
C          COORD(I+TWICENR)=COORD(I)
28    CONTINUE
C
C*****
C
C      THIS SECTION SETS UP A CUTOFF POINT REFERRING TO THE NUMBER OF
C      VORTEX RINGS THAT OCCUR ON THE RIGHT AND LEFT SIDE OF THE SYSTEM.
C      THESE CUTOFF POINTS ARE LATER USED TO DETERMINE THE DISTANCES
C      BETWEEN POINTS AT WHICH THE AXIAL VELOCITIES ARE CALCULATED AND
C      THE APPROPRIATE VORTEX SYSTEM CENTERLINE.
C
C*****
C
C
60    IF(TNR.EQ.36) THEN
      RS=18
      LS=19
      ENDIF
      IF(TNR.EQ.48) THEN
      RS=20
      LS=21
      ENDIF
      IF(TNR.EQ.68) THEN
      RS=34
      LS=35
      ENDIF
      IF(TNR.EQ.72) THEN
      RS=36
      LS=37
      ENDIF
      IF(TNR.EQ.128) THEN
      RS=64
      LS=65
      ENDIF
      IF(TNR.EQ.132) THEN
      RS=66
      LS=67
      ENDIF
      IF(TNR.EQ.136) THEN
      RS=68
      LS=69
```

ORIGINAL PAGE IS
OF POOR QUALITY

```

      ENDIF
C
C=====
C
C THIS SECTION IS THAT IN WHICH THE ACTUAL AXIAL VELOCITY COMPONENTS
C ARE CALCULATED. THE SECTION CONSISTS OF A SERIES OF IF/THEN STATE-
C MENTS AND TWO NESTED DO LOOPS.
C THE PURPOSE OF THE IF/THEN STATEMENTS IS TO SET THE CORRECT RELATION-
C SHIPS REGARDING THE DISTANCES THAT ARE NEEDED FOR THE VELOCITY CAL-
C ULATIONS.
C THE CALCULATION BEGINS AT A POINT 35 FEET FROM THE AIRCRAFT LONGITUDINAL
C CENTERLINE AND ENDS AT A POINT 35 FEET ON THE OPPOSITE SIDE OF THE
C CENTERLINE. THE IF/THEN STATEMENTS SET THE PROPER DISTANCES BETWEEN
C EACH SUCCESSIVE POINT, WHERE THE VELOCITIES ARE TO BE CALCULATED, AND
C THE CENTERLINES OF THE TWO RESPECTIVE VORTEX SYSTEM CENTERLINES
C (+/-16.0833 FT). THE DISTANCES ARE ALSO DEPENDENT ON WHICH SET OF
C VORTEX RINGS ARE BEING CONSIDERED RELATIVE TO THE LOCATION OF THE
C POINT AT WHICH THE VELOCITIES ARE BEING CALCULATED.
C WITH THE PROPER RELATIVE DISTANCES ESTABLISHED, THE RATIOS X (RING
C DOWNSTREAM POSITION TO RING RADIUS) AND R (DISTANCE, FROM THE POINT TO
C THE CURRENT VORTEX RING SYSTEM CENTERLINE, TO RING RADIUS) ARE DETER-
C MINED AND THE VELOCITY CALCULATION IS CARRIED OUT.
C IF AN ICE HOVER CONDITION IS BEING ANALYZED, AN IF/THEN STATEMENT
C CHANGES THE CIRCULATION SO AS TO MAKE IT NEGATIVE IN THE REFLECTED
C VORTEX SYSTEM.
C FINAL VELOCITY RESULTS ARE STORED IN THE DOUBLELY SUBSCRIPTED ARRAY
C V(M,N), ACCOMODATING VELOCITIES FROM 71 POINTS AND TMR VORTEX RINGS.
C
C=====
C
C
C=====

      L=-35
      DO 65 M=1,71
      C
      DO 70 N=1,TMR
      RAD=16.0833
      IF((L.LT.0).AND.(N.LE.RS)) THEN
      J=L
      RAD=16.0833
      ENDIF
      IF((L.LE.-17).AND.(N.GE.RS)) THEN
      J=L
      RAD=16.0833
      ENDIF
      IF((L.GE.-16).AND.(L.LT.0).AND.(N.GE.RS)) THEN
      J=L
      RAD=16.0833
      ENDIF
      IF((L.GT.0).AND.(N.GE.RS)) THEN
      J=L
      RAD=16.0833
      ENDIF
      IF((L.LE.16).AND.(L.GT.0).AND.(N.LE.RS)) THEN
      J=L
      RAD=16.0833
      ENDIF
      IF((L.GE.17).AND.(N.LE.RS)) THEN
      J=L

```

ORIGINAL PAGE IS
OF POOR QUALITY

```

RAD=-16.0833
ENDIF
IF(L.EQ.0) THEN
J=L
RAD=16.0833
ENDIF
X=COORD(N)/RR(N)
R=(RAD+J)/RR(N)
S=(4.*R)/(X**2.+((R+1.)**2.))
T=ALOG(4./((1.-S)**.5))
U=T+((T-1.)/4.)*(1.-S)+(9./64.)*(T-(7./6.))*(1.-S)**2.
E=1.+(.5*(T-.5)*(1.-S))+(3./16.)*(T-(13./12.))*(1.-S)**2.
B=1./((X**2.+((R+1.)**2.))**.5
C=-(1.+((2.*(R-1.))/(X**2.+((R-1.)**2.))))
D=U+C*E
P=B*D
A=ABS(A)
IF((HOVERD.NE.0.0).AND.(N.GT.NUMRING).AND.(N.LE.TWICNR)
+.ON.
+.((HOVERD.NE.0.0).AND.(N.GT.THREENR).AND.(N.LE.TNR)) THEN
A=A
ENDIF
CIRC=A/(2.*3.14159*RR(N))
V(M,N)=CIRC*P
70  CONTINUE
C
L=L+1
65  CONTINUE
C
C*****
C
C THE NEXT NESTED DO LOOPS PERFORM THE TASK OF SUMMING THE VELOCITIES
C AT EACH POINT DUE TO EACH OF THE RINGS. HENCE, FROM HERE, THE TOTAL
C VELOCITIES AT EACH OF 71 POINTS ARE OBTAINED AND STORED IN THE ARRAY
C VTOT(J).
C
C*****
C
DO 75 J=1,71
    DO 76 I=1,TNR
        VTOT(J)=VTOT(J)+V(J,I)
76  CONTINUE
WRITE(*,88) J,VTOT(J)
88  FORMAT(/,2X,5HVTOT(,12.2H)=,F6.2,3X,6HFT/SEC)
75  CONTINUE
C
C*****
C
C THIS SECTION OUTPUTS THE CHOSEN THRUST COEFFICIENT (CT), ROTOR HEIGHT
C ABOVE GROUND TO ROTOR DIAMETER RATIO (D/D), THE ASSIGNED VALUE OF THE
C VORTEX RING SPACING FACTOR (K) AND THE RESULTING NUMBER OF VORTEX RINGS
C (TNR).
C
C*****

```

```

C
C
C LAC=25.
C BACTRD=ZAC/LAC
C WRITE(6,33)CT,RACTRD
33 FORMAT(//,' FOR CT=' ,F6.5,' ,A TRUE B/D=' ,F4.2)
IF(BOVERD.EQ.0.0) THEN
WRITE(6,34)
34 FORMAT(' (B/D=0.00 SIGNIFIES AN OCE BOVER CONDITION)')
ENDIF
WRITE(6,85)K,TNR
85 FORMAT(' K=' ,F4.3,' AND' ,IX,13,' VORTEX RINGS')
C
C ****
C
C THE FOLLOWING DO LOOP PERFORMS A SERIES OF TASKS. FIRST, ONLY THE
C COMPUTED VELOCITIES THAT LIE BETWEEN THE ROTOR CENTERLINES ARE CONSIDERED.
C THIS BEING WHERE THE ACTUAL AIRCRAFT WING IS. STARTING ON THE LEFT
C BAND SIDE, EACH TWO SUCCESSIVE VELOCITIES ARE AVERAGED. THE AVERAGED
C VELOCITIES THEN BEING USED TO COMPUTE A DOWNLOAD. IF THE AREAS WHERE
C THE VELOCITIES OCCUR ARE IN THE VICINITY OF THE WINGS AND NOT THE
C FUSELAGE, THE PREDETERMINED DRAC COEFFICIENT IS USED. IF THE AREAS
C WHERE THE VELOCITIES OCCUR ARE IN THE VICINITY OF THE FUSELAGE, THE
C DRAC COEFFICIENT IS ASSUMED TO BE 1, FOR WANT OF A BETTER VALUE.
C TWO IF/THEN STATEMENTS TAKE CARE OF THIS DISTINCTION. THE DOWNLOAD
C COMPONENTS ARE THEN SUMMED TO ARRIVE AT A TOTAL DOWNLOAD. THIS FINAL
C VALUE (IN POUNDS) IS THEN OUTPUT ALONG WITH THE CHOSEN FLAP SETTING.
C
C ****
C
C DO 699 I=20,52
C     VBAR=(VTOT(I)+VTOT(I+1))/2.0
C     IF((I.GE.33).AND.(I.LE.39)) THEN
C         DWNLDD=.5*.002378*VBAR**2.0*5.25
C     ENDIF
C     IF((I.LT.33).OR.(I.GT.39)) THEN
C         DWNLDD=.5*.002378*VBAR**2.0*5.25*CD.
C     ENDIF
C     DWNLD2=DWNLD2+DWNLDD
699  CONTINUE
C     WRITE(6,399)DWNLD2
399  FORMAT(' THE XV-15 ROTOR DOWNLOAD IS =' ,F8.3,' LB.')
C     WRITE(6,589)FLAPSET,CD
589  FORMAT(' FOR A FLAP SETTING OF' ,IX,13,' DEGREES (CD=' ,F4.2,')')
C
C ****
C
C THE LAST SECTION CONSISTS OF THREE IF/THEN STATEMENTS AND HANDLES
C THE TASK OF CALCULATING AND OUTPUTTING THE FINAL TOTAL DOWNLOAD AS
C A PERCENTAGE OF TOTAL ROTOR THRUST. SINCE THE TOTAL ROTOR THRUST
C PRODUCED IS A FUNCTION OF THE THRUST COEFFICIENT, THE PREREQUISITE
C FOR THE IF/THEN STATEMENTS IS THE THRUST COEFFICIENT. EACH IF/THEN
C STATEMENT DIVIDES THE TOTAL DOWNLOAD BY THE APPROPRIATE TOTAL THRUST
C AND OUTPUTS THIS PERCENTAGE VALUE.
C

```

ORIGINAL PAGE IS
OF POOR QUALITY

```
C
C*****C*****
C
C      IF(CT.EQ..0094) THEN
PRCNDLI=(DWNL02/12956.62)*100.
WRITE(6,400)
400  FORMAT(' BASED ON A THRUST COEFFICIENT OF .0094')
WRITE(6,401)PRCNDLI
401  FORMAT(' THIS REPRESENTS',1X,F6.3,' % OF TOTAL ROTOR THRUST')
ENDIF
C
C      IF(CT.EQ..01) THEN
PRCNDLI=(DWNL02/13783.64)*100.
WRITE(6,403)
403  FORMAT(' BASED ON A THRUST COEFFICIENT OF .01')
WRITE(6,404)PRCNDLI
404  FORMAT(' THIS REPRESENTS',1X,F6.3,' % OF TOTAL ROTOR THRUST')
ENDIF
C
C      IF(CT.EQ..0105) THEN
PRCNDLI=(DWNL02/14472.82)*100.
WRITE(6,406)
406  FORMAT(' BASED ON A THRUST COEFFICIENT OF .0105')
WRITE(6,407)PRCNDLI
407  FORMAT(' THIS REPRESENTS',1X,F6.3,' % OF TOTAL ROTOR THRUST')
ENDIF
C
STOP
END
```

Appendix F
Calibration Version of Model Rotor
Computer Program

C
C
C THIS PROGRAM IS DESIGNED TO SIMULATE THE MODEL ROTOR SYSTEM TEST
C PERFORMANCE THROUGH THE USE OF A VORTEX RING ANALYSIS. THE PROGRAM
C IS BASED ON A ROTOR THRUST COEFFICIENT OF .0075 AND TIP SPEED OF
C 83.25 FT/SEC. THIS PARTICULAR PROGRAM VERSION WAS DESIGNED TO
C CALIBRATE THE VORTEX RING SPACING FACTOR (K). THE VALUE FOR K IS
C AN INPUT PARAMETER IN THIS PROGRAM AND IS VARIED UNTIL AN AVERAGE
C INFLOW VELOCITY THROUGH THE ROTOR DISK THAT AGREES WITH THAT
C PREDICTED BY MOMENTUM THEORY IS OBTAINED. THE POINTS AT WHICH THE
C VELOCITIES ARE CALCULATED LIE ALONG A LINE WHICH IS COINCIDENTAL
C WITH THE ROTOR PLANE.
C
C*****
C
C*****
C
C LIST OF VARIABLES:
C
C K.....VORTEX RING SPACING FACTOR
C H.....ROTOR SPEED (SEC/REV)
C F(I)....TIME BETWEEN VORTEX RINGS (SEC)
C ET(I)....CORRECTED TIME BETWEEN VORTEX RINGS (SEC)
C (K*F(I))
C Z(I).....THE POSITION OF EACH VORTEX RING, DOWN-
C STREAM OF THE ROTOR DISK, AS A FUNCTION OF
C CORRECTED TIME (FT)
C RR(I).....VORTEX RING RADIUS (FT)
C (A FUNCTION OF ROTOR GEOMETRY AND RING
C DOWNSTREAM POSITION)
C TNR.....THE TOTAL NUMBER OF VORTEX RINGS CONSIDERED
C IN THE ANALYSIS
C A.....THE VORTEX/RING CIRCULATION (FT**2/SEC)
C CT.....THRUST COEFFICIENT (THRUST/(RHO*AREA*V1**2))
C POINT.....THE DISTANCE BETWEEN THE ROTOR AXIS AND THE
C POINT WHERE THE AXIAL VELOCITIES ARE BEING
C CALCULATED (FT)
C RAD.....THE ABSOLUTE VALUE OF POINT (FT)
C X.....THE RATIO OF VORTEX RING DOWNSTREAM
C POSITION TO RING RADIUS (-Z(I)/RR(I))
C R.....THE RATIO OF POINT TO THE RING RADIUS
C (RAD/RR(I))
C S,T,U,E,B,C,CIRC.....COMPONENTS OF THE EQUATION USED TO
C DETERMINE THE AXIAL VELOCITY DUE TO EACH
C RING (FROM "AERODYNAMICS OF PROPULSION"
C EUCHEMANN & WEBER, 1953)
C P,D.....INTERMEDIATE STORAGE/VARIABLES
C V(M,N).....THE COMPONENT OF THE AXIAL VELOCITY AT
C POINT M DUE TO RING N (FT/SEC)
C VTOT(I).....THE TOTAL AXIAL VELOCITY AT EACH OF 25
C POINTS DUE TO SUMMING THE COMPONENTS FROM
C EACH VORTEX RING (FT/SEC)
C VAVG.....THE SUM OF THE AXIAL VELOCITIES ALONG THE
C ROTOR DISK (FT/SEC)
C VDISK.....THE AVERAGE INFLOW VELOCITY ALONG THE ROTOR
C DISK (FT/SEC)

```

C
C
C*****  

C
C      REAL K,KT(72)
C      INTEGER TNR
C      DIMENSION Z(144),F(36),RR(144),VTOT(71),V(71,144)
C
C*****  

C
C      THE VALUE TO BE USED FOR THE VORTEX RING SPACING FACTOR (K) IS
C      FIRST READ IN
C
C*****  

C
C      WRITE(6,4)
4      FORMAT('WHAT K VALUE WILL BE USED?')
READ(5,5)K
5      FORMAT(F8.7)
C
C*****  

C
C      NEXT, BASED ON A ROTOR SPEED OF 700 RPM, THE TIME SPACING OF
C      THE VORTEX RINGS IS CALCULATED USING THE RING SPACING FACTOR (K).
C
C*****  

C
C      H=.0057
DO 20 I=1,72
      F(I)=I*H/2.0
      KT(I)=K*F(I)
20  CONTINUE
C
C*****  

C
C      A FIFTH ORDER INTERPOLATING POLYNOMIAL IS USED TO DETERMINE THE
C      DOWNSTREAM POSITION OF EACH VORTEX RING AS A FUNCTION OF TIME.
C      EACH VORTEX RING'S RADIUS IS ALSO CALCULATED AS A FUNCTION OF
C      RING DOWNSTREAM POSITION.
C
C*****  

C
25  DO 40 I=1,72
      Z(I)=3.3421*KT(I)**5.+15.5269*KT(I)**4.-24.8107*KT(I)
      +    **3.+12.8299*KT(I)**2.+7.2438*KT(I)
      RR(I)=.80274*SQRT(I/.5*(2.-EXP(-1.0476*Z(I)))))
40  CONTINUE
TNR=72.
C

```

ORIGINAL PAGE IS
OF POOR QUALITY

```

C
C
C THE VALUES OF THRUST COEFFICIENT (CT), RING CIRCULATION (A) AND THE
C POSITION OF THE FIRST POINT, WITH RESPECT TO THE ROTOR AXIS, (POINT),
C ARE NOW ENTERED.
C
C
C*****24      CT=.0075
C*****      A=2.226
C*****      POINT=-1.5
C
C
C*****TWO DO LOOPS ARE NOW USED TO CALCULATE EACH VORTEX RING'S AXIAL
C*****VELOCITY COMPONENT AT EACH POINT OF INTEREST. THE INNER LOOP
C*****CALCULATES THE VELOCITIES FROM EACH OF THE RINGS AND THE OUTER
C*****LOOP INCREMENTS THE POINT AT WHICH THE VELOCITIES ARE CALCULATED.
C
C
C*****DO 65 N=1,25
C
C
C*****DO 70 N=1,TNR
C*****      IF(POINT.LT.0.) RAD=-POINT
C*****      IF(POINT.GT.0.) RAD=POINT
C*****      X=-Z(N)/RR(N)
C*****      R=RAD/RR(N)
C*****      S=(4.*R)/(X**2.+(R+1.)**2.)
C*****      T=ALOC(4./SQR(1.-S))
C*****      U=T+((T-1.)/4.)*(1.-S)+(9./64.)*(T-(7./6.))*(1.-S)**2.
C*****      E=1.+(.5*(T-1.)*(1.-S))+(3./16.)*(T-(13./12.))*(1.-S)**2.
C*****      B=1./SQR(X**2.+(R+1.)**2.)
C*****      C=-(1.+((2.*(R-1.))/(X**2.+(R-1.)**2.)))
C*****      D=U+C*E
C*****      P=B*D
C*****      CIRC=A/(2.*3.14156*RR(N))
C*****      V(M,N)=CIRC*P
C*****CONTINUE
C
C
C*****POINT=POINT+.125
C*****CONTINUE
C
C
C*****THE VELOCITY COMPONENTS DUE TO EACH OF THE VORTEX RINGS ARE NOW
C*****SUMMED TO ARRIVE AT A TOTAL AXIAL VELOCITY AT EACH OF THE 25 POINTS
C*****OF INTEREST.
C

```

```
C
C
C      DO 73 J=1,25
C
C      DO 80 I=1,TNR
C          VTOT(J)=VTOT(J)+V(J,I)
C          CONTINUE
C
C      75  CONTINUE
C
C
C*****THE TOTAL AXIAL VELOCITY AT EACH POINT OF INTEREST IS NOW PRINTED
C*****OUT ALONG WITH THE ASSOCIATED VALUES OF THRUST COEFFICIENT (CT),
C*****VORTEX RING SPACING FACTOR AND THE TOTAL NUMBER OF VORTEX RINGS
C*****USED IN THE VELOCITY CALCULATIONS.
C
C
C      WRITE(6,33)CT
33    FORMAT(' FOR A THRUST COEFFICIENT OF CT=' ,F6.5)
C      WRITE(6,85)K,TNR
85    FORMAT(IX,' K=' ,F8.7,' AND' ,IX,12,' VORTEX RINGS')
C      WRITE(6,90)
90    FORMAT(IX,' THE TOTAL AXIAL VELOCITY AT EACH POINT ALONG A LINE')
C      WRITE(6,95)
95    FORMAT(IX,' COINCIDENTAL WITH THE PLANE OF THE ROTOR IS:' )
C
C      DO 97 J=1,25
C          WRITE(6,96) J,VTOT(J)
96    FORMAT(IX,5HEVTOT(1,12,2H)=.G12.5.6EFT/SEC)
C          CONTINUE
C
C
C*****SINCE FOR CALIBRATION PURPOSES THE AVERAGE VELOCITY ALONG THE
C*****ROTOR DISK IS WHAT'S OF PRIME IMPORTANCE, THAT VALUE IS NOW
C*****CALCULATED AND OUTPUT.
C
C
C      DO 100 I=4,13
C          VAVG=VAVG+VTOT(I)
100   CONTINUE
C
C          VDISK=VAVG/10.0
C          WRITE(6,110)VDISK
110   FORMAT(IX,' THE AVERAGE INFLOW VELOCITY IS' ,IX,F0.5,' FT/SEC')
```

C

STOP
END

Appendix G
Download Version of Model Rotor
Computer Program

ORIGINAL PAGE IS
OF POOR QUALITY

```

C
C
C THIS PROGRAM IS DESIGNED TO SIMULATE THE MODEL ROTOR SYSTEM TEST
C PERFORMANCE THROUGH THE USE OF A VORTEX RING ANALYSIS. THE PROGRAM
C IS BASED ON A ROTOR THRUST COEFFICIENT OF .0075 AND TIP SPEED OF
C 83.25 FT/SEC. UTILIZING THE PREDETERMINED VORTEX RING SPACING
C FACTOR K. THIS PROGRAM COMPUTES A DOWNLOAD BASED ON THE MODEL WING
C (CHORD = 4.7 IN., SPAN = 16.81 IN.) AT A POSITION 1.5 IN. DOWN-
C STREAM OF THE ROTOR PLANE. THE COMPUTED AXIAL VELOCITIES ARE USED
C TO DETERMINE A VALUE OF DYNAMIC PRESSURE ( $\rho$ ). WHICH WHEN MULTIPLIED
C BY A SECTIONAL SURFACE AREA GIVES A DOWNLOAD COMPONENT.
C
C ****
C
C LIST OF VARIABLES:
C
C K.....VORTEX RING SPACING FACTOR
C N.....ROTOR SPEED (SEC/REV)
C F(I)....TIME BETWEEN ROTOR BLADE PASSAGES (SEC/REV)
C ET(I)....CORRECTED TIME BETWEEN VORTEX RING SHEDDING
C (K*F(I)) (SEC/REV)
C Z(I)....THE POSITION OF EACH VORTEX RING, DOWN-
C STREAM OF THE ROTOR DISK, AS A FUNCTION OF
C CORRECTED TIME (FT)
C COORD(I)....THE DOWNSTREAM POSITION OF THE VORTEX RINGS
C WITH RESPECT TO A LINE THAT IS COINCIDENTAL
C WITH THE MODEL ROTOR'S WING (FT)
C RR(I)....VORTEX RING RADIUS (FT)
C (A FUNCTION OF ROTOR GEOMETRY AND VORTEX RING
C DOWNSTREAM POSITION)
C NUMRINC....THE NUMBER OF VORTEX RINGS, FOR AN ICE ROVER
C CONDITION, THAT SATISFIES THE PRESCRIBED ROTOR HEIGHT
C ABOVE GROUND PLANE TO ROTOR DIAMETER RATIO
C TNR....THE TOTAL NUMBER OF VORTEX RINGS CONSIDERED
C IN THE ANALYSIS
C A.....THE VORTEX RING CIRCULATION (FT**2/SEC)
C CT.....THRUST COEFFICIENT (THRUST/(RHO*AREA*VT*P**2))
C POINT....THE DISTANCE BETWEEN THE ROTOR AXIS AND THE
C POINT WHERE THE AXIAL VELOCITIES ARE BEING
C CALCULATED (FT)
C RAD.....THE ABSOLUTE VALUE OF POINT (FT)
C X.....THE RATIO OF VORTEX RING DOWNSTREAM
C POSITION TO RING RADIUS (Z(I)/RR(I))
C R.....THE RATIO OF POINT TO THE RING RADIUS
C (RAD/RR(I))
C S.T.U.E.B.C.CIRC..COMPONENTS OF THE EQUATION USED TO
C DETERMINE THE AXIAL VELOCITY DUE TO EACH
C RING (FROM: "AERODYNAMICS OF PROPULSION",
C KUCHEMANN & WEBER, 1953)
C P,D.....INTERMEDIATE STORAGE VARIABLES
C V(M,N)....THE COMPONENT OF THE AXIAL VELOCITY AT
C POINT M DUE TO RING N (FT/SEC)
C VTOT(I)....THE TOTAL AXIAL VELOCITY AT EACH OF 25
C POINTS DUE TO SUMMING THE COMPONENTS FROM

```

```

C          EACH VORTEX RING (FT/SEC)
C  VBAR.....THE AVERAGE INFLOW VELOCITY BETWEEN TWO
C          SUCCESSIVE POINTS AT WHICH THE AXIAL
C          VELOCITIES WERE CALCULATED (FT/SEC)
C  DVNLD1.....THE DOWNLOAD COMPONENT FOR THE AREA BETWEEN
C          TWO SUCCESSIVE POINTS AT WHICH THE AXIAL
C          VELOCITIES WERE CALCULATED (LB)
C  DVNLD2.....THE SUM OF THE INDIVIDUAL DOWNLOAD
C          COMPONENTS. I.E., THE TOTAL DOWNLOAD (LB)
C  PRCNTDL.....THE PERCENT OF ROTOR THRUST THAT IS DOWNLOAD
C
C*****=====
C
C
REAL K,KT(72)
INTEGER Y,TNR
DIMENSION Z(144),COORD(144),F(36),RR(144),VTOT(71),V(71,144)
C
C*****=====
C
C
C DUE TO THE FACT THAT THREE DIFFERENT ROTOR HEIGHT TO ROTOR
C DIAMETER RATIOS WERE RUN WITH THE MODEL SYSTEM, THREE H/D
C RATIOS CAN BE ANALYZED WITH THIS PROGRAM. TWO ARE IN GROUND
C EFFECT (ICE) CONDITIONS, H/D=0.5 & 1.0, AND ONE IS AN OUT
C OF GROUND EFFECT (OCE) CONDITION, H/D=INFINITY. THE SELECTION
C FOR THE GROUND EFFECT CONDITION TO BE ANALYZED IS MADE HERE.
C
C*****=====
C
C
C
16  WRITE(6,16)
FORMAT(' WHAT H/D RATIO WILL BE USED?')
14  WRITE(6,14)
FORMAT(' (0.5,1.0, OR OCE HOVER)?')
17  WRITE(6,17)
FORMAT(' (ENTER 0 FOR OCE HOVER)')
READ(5,18)HOVERD
18  FORMAT(C12.3)
C
C*****=====
C
C
C NEXT, BASED ON A ROTOR SPEED OF 1000 RPM, THE TIME SPACING OF
C THE VORTEX RINGS IS CALCULATED USING THE RING SPACING FACTOR (K).
C
C*****=====
C
C
K=.41946
B=.0857
DO 20 I=1,72
      F(I)=I*B/2.0
      KT(I)=K*F(I)
20  CONTINUE

```

```

C
C
C      A FIFTH ORDER INTERPOLATING POLYNOMIAL IS USED TO DETERMINE THE
C      DOWNSTREAM POSITION OF EACH VORTEX RING AS A FUNCTION OF TIME.
C      IF ONE OF THE ICE HOVER CONDITIONS IS BEING ANALYZED THE CALCULATION
C      IS TERMINATED AT THE RING THAT COINCIDES WITH THE GROUND PLANE AND
C      CONTROL IS TRANSFERRED TO STATEMENT 26. EACH VORTEX RING'S RADIUS
C      IS ALSO CALCULATED AS A FUNCTION OF DOWNSTREAM POSITION.
C
C=====
C
C
23    DO 40 I=1,72
        Z(I)=3.5421*KT(I)**5.+15.5269*KT(I)**4.-24.8167*KT(I)
        + **3.+12.8299*KT(I)**2.+7.2430*KT(I)
        RR(I)=.88274*SQRT(1./(.5*(2.-EXP(-1.6476*Z(I)))))
        COORD(I)=Z(I)-.125
        IF((HOVERD.EQ.0.5).AND.(Z(I).GE.1.135).OR.
        +(HOVERD.EQ.1.0).AND.(Z(I).GE.2.27))THEN
          NUMRING=1
          GO TO 26
        ENDIF
40    CONTINUE
        TNR=72.
        GO TO 24
C
C=====
C
C      IN THE EVENT THAT ONE OF THE ICE HOVER CONDITIONS IS BEING ANALYZED
C      THIS SECTION FORMS THE MIRROR IMAGE OF THE PREDETERMINED VORTEX
C      RING SYSTEM. IF THE OCE HOVER CONDITION IS BEING ANALYZED THIS
C      SECTION IS BYPASSED AND CONTROL IS TRANSFERRED TO STATEMENT 24.
C
C=====
C
C
26    Y=NUMRING+1
        Z(Y)=Z(NUMRING)
        RR(Y)=RR(NUMRING)
        COORD(Y)=COORD(NUMRING)
C
C
27    DO 27 I=2,NUMRING
        LOPE=I+NUMRING
        LIP=Y-I
        Z(LOPE)=Z(Y)+(Z(Y)-Z(LIP))
        RR(LOPE)=RR(LIP)
        COORD(LOPE)=Z(LOPE)-.1979
27    CONTINUE
C
C=====
C
C      THE VALUE OF THE TOTAL NUMBER OF RINGS..(TNR) FOR ICE BOVERS. THRUST

```

ORIGINAL PAGE IS
OF POOR QUALITY

C COEFFICIENT (CT). RING CIRCULATION (A) AND THE POSITION OF THE FIRST
C POINT, WITH RESPECT TO THE ROTOR AXIS..(POINT), ARE NOW ENTERED.

C
C
C*****
C

24 TMR=2.*NUMRING
CT=.0075
A=2.226
POINT=-1.5

C
C
C*****
C

C TWO DO LOOPS ARE NOW USED TO CALCULATE EACH VORTEX RING'S AXIAL
C VELOCITY COMPONENT AT EACH POINT OF INTEREST. THE INNER LOOP
C CALCULATES THE VELOCITIES FROM EACH OF THE RINGS AND THE OUTER
C LOOP INCREMENTS THE POINT AT WHICH THE VELOCITIES ARE CALCULATED.
C
C
C*****
C

DO 65 N=1,25

C
C

DO 70 N=1,TMR
IF(POINT.LT.0.) RAD=-POINT
IF(POINT.GT.0.) RAD=POINT
X=-COORD(N)/RR(N)
R=RAD/RR(N)
S=(4.*R)/(X**2.+(R+1.)**2.)
T=ALOC(4./SQRT(1.-S))
U=T*((T-1.)/4.)*(1.-S)+(9./64.)*(T-(7./6.))*(1.-S)**2.
E=1.+(.5*(T-.5)*(1.-S))+(3./16.)*(T-(13./12.))*(1.-S)**2.
B=1./SQRT(X**2.+(R+1.)**2.)
C=-(1.+((2.*(R-1.))/(X**2.+(R-1.)**2.)))
D=U+C*E
P=B*D
A=ABS(A)
IF((HOVERDINE.0.00).AND.(N.GE.Y)) THEN
A=-A
ENDIF
CIRC=A/(2.*3.14156*RR(N))
V(M,N)=CIRC*P
CONTINUE

70
C
C
POINT=POINT+.125
CONTINUE

C
C
C*****
C

C THE VELOCITY COMPONENTS DUE TO EACH OF THE VORTEX RINGS ARE NOW
C SUMMED TO ARRIVE AT A TOTAL AXIAL VELOCITY AT EACH OF THE 25 POINTS
C OF INTEREST.

C

```

C
C*****DO 73 J=1,25
C
C      DO 80 I=1,TNR
C          VTOT(J)=VTOT(J)+V(J,I)
C          CONTINUE
C
C      73   CONTINUE
C
C*****THE TOTAL AXIAL VELOCITY AT EACH POINT OF INTEREST IS NOW PRINTED
C      OUT ALONG WITH THE ASSOCIATED VALUES OF ROTOR HEIGHT TO ROTOR
C      DIAMETER RATIO, THRUST COEFFICIENT, VORTEX RING SPACING FACTOR AND
C      THE TOTAL NUMBER OF VORTEX RINGS USED IN THE VELOCITY CALCULATIONS.
C
C*****WRITE(6,33)CT,HOVERD
33    FORMAT(' CT',F6.5,' B/D',F4.2)
IF (HOVERD.EQ.0) THEN
WRITE(6,34)
34    FORMAT(' (B/D=0.00 SIGNIFIES AN OGE HOVER CONDITION)')
ENDIF
WRITE(6,85)K,TNR
85    FORMAT(IX,' FOR K=',F8.7,' AND ',IX,12,' VORTEX RINGS')
WRITE(6,90)
90    FORMAT(IX,' THE TOTAL AXIAL VELOCITY AT EACH POINT ALONG A LINE')
WRITE(6,95)
95    FORMAT(IX,' COINCIDENT WITH THE PLANE OF THE WING IS:')
C
C      DO 97 J=1,25
C          WRITE(6,96) J,VTOT(J)
96    FORMAT(1,2X,5HVTOT(.12,2H)=,G12.5,6HFT/SEC)
97    CONTINUE
C
C*****DOWNLOAD COMPONENTS ARE NOW COMPUTED BASED ON THE AVERAGE AXIAL
C      VELOCITY BETWEEN TWO POINTS OF CONSIDERATION. THE TOTAL DOWN-
C      LOAD IS THEN COMPUTED AS THE SUM OF THE COMPONENTS.
C
C*****DO 699 I=1,12
699   VBAR=(VTOT(I)+VTOT(I+1))/2.0
      DNLDS=.5*.002378*VBAR**2.0*.04896*1.98

```

ORIGINAL PAGE IS
OF POOR QUALITY

```
DWNLD2=DWNLD2+DWNLD1
499    CONTINUE
C
C
C*****                                                 *****
C
C      THE FINAL RESULT FOR THE MODEL ROTOR SYSTEM THEORETICAL DOWNLOAD IS
C      NOW OUTPUT.
C
C
C*****                                                 *****
C
C      WRITE(6,390)DWNLD2:
390      FORMAT(/, ' THE MODEL ROTOR DOWNLOAD IS ',C12.5,' LB.')
      PRCNTDL=(DWNLD2/6.5)*100
      WRITE(6,395)
395      FORMAT(' BASED ON A THRUST COEFFICIENT OF .0075 ')
      WRITE(6,400)PRCNTDL
400      FORMAT(' THIS REPRESENTS',IX,F5.3,' % OF ROTOR THRUST')
C
C
      STOP
      END
```